



# **BRNO UNIVERSITY OF TECHNOLOGY**

VYSOKÉ UČENÍ TECHNICKÉ V BRNĚ

## **FACULTY OF MECHANICAL ENGINEERING**

FAKULTA STROJNÍHO INŽENÝRSTVÍ

## **INSTITUTE OF SOLID MECHANICS, MECHATRONICS AND BIOMECHANICS**

ÚSTAV MECHANIKY TĚLES, MECHATRONIKY A BIOMECHANIKY

# **ANALYSIS OF TRANSFER MATRIX METHOD USING FOR CALCULATION OF ELECTRICAL MACHINES ROTOR WITH INFLUENCE OF MAGNETIC PULL**

ANALÝZA VYUŽITÍ METODY PŘENOSOVÝCH Matic PRO MECHANICKÝ VÝPOČET ROTORU  
ELEKTRICKÝCH STROJŮ S UVÁŽENÍM MAGNETICKÉHO TAHU

### **MASTER'S THESIS**

DIPLOMOVÁ PRÁCE

#### **AUTHOR**

AUTOR PRÁCE

**Bc. JAN TOBIÁŠ**

#### **SUPERVISOR**

VEDOUCÍ PRÁCE

**doc. Ing. RADEK VLACH, Ph.D.**

**BRNO 2022**

# Assignment Master's Thesis

Institut: Institute of Solid Mechanics, Mechatronics and Biomechanics  
Student: **Bc. Jan Tobiáš**  
Degree program: Engineering Mechanics and Biomechanics  
Branch: Engineering Mechanics  
Supervisor: **doc. Ing. Radek Vlach, Ph.D.**  
Academic year: 2021/22

As provided for by the Act No. 111/98 Coll. on higher education institutions and the BUT Study and Examination Regulations, the director of the Institute hereby assigns the following topic of Master's Thesis:

## **Analysis of transfer matrix method using for calculation of electrical machines rotor with influence of magnetic pull**

### **Recommended bibliography:**

ZIENKIEWICZ, O.C., TAYLOR, R.L.: The Finite Element Method. Butterworth Heinemann, London, 2000

BITTNAR, Z., ŠEJNOHA, J.: Numerické metody mechaniky 1, 2. Vydavatelství ČVUT, Praha, 1992

BATHE K.-J.: Finite Element Procedures. Prentice Hall, 1996

SLAVÍK, J., STEJSKAL V., ZEMAN V.: Základy dynamiky strojů, 2000

Deadline for submission Master's Thesis is given by the Schedule of the Academic year 2021/22

In Brno,

L. S.

---

prof. Ing. Jindřich Petruška, CSc.  
Director of the Institute

---

doc. Ing. Jaroslav Katolický, Ph.D.  
FME dean

## Summary

This master thesis is dealing with modeling of the rotor system based on the numerical transfer matrix calculations. This method is suitable for fast analysis of beam bodies to observe the resulting deflection and critical speed in regard to the initial circumstances. The bearing stiffness is a significant input factor that affects the outcomes of the analysis, especially the critical speed the rotor system.

First of all, the available approaches to analyze the bended beam bodies are discussed focused on explanation of the transfer matrix algorithm. After that, the approach to estimate the bearing stiffness based on the Hertz contact theory is presented. Further, a brief explanation is given about the heat arising in the rotor bearings.

The following chapters are focused on description of the software solver for rotor system analysis based on the transfer matrix method, considering the bearing stiffness estimation based on Hertz contact theory, with possible calculations of the induced bearing heat losses.

In the end, the practical use of the developed software is presented with the analysis of the obtained results of the rotor deflection, critical speed, and bearing power loss. There is also discussed a comparison of the different bearing stiffness estimation with the impact to the computation outcomes, especially on the rotor critical speed, followed by comparison conclusion implementation into rotor system analysis.

## Abstrakt

Tato diplomová práce se zabývá modelováním rotorových soustav pomocí numerické metody přenosových matic. Tato metoda je pro svou časovou efektivitu vhodná pro výpočty ohýbaných nosníků a analýzu výsledného průhybu a kritických otáček dané rotorové soustavy s ohledem na vstupní počáteční podmínky. Jedním z významných vstupních parametrů takovéto analýzy je tuhost ložisek rotoru a její vliv na výsledné kritické otáčky rotoru.

Nejdříve jsou prezentovány dostupné výpočtové metody pro ohýbané nosníky se zaměřením na vysvětlení principu metody přenosových matic. Následuje nastínění výpočtu tuhosti ložiska na základě teorie Hertzova kontaktního tlaku. Dále je stručně vysvětlen princip výpočtu tepelných ztrát generovaných v ložiscích rotoru.

Další kapitoly se zabírají popisem navrženého řešice rotorových systémů, založeného na metodě přenosových matic, s možností stanovit tuhost ložiska na základě Hertzova kontaktního tlaku a možností stanovit tepelné ztráty v ložiscích rotoru.

Nakonec je ukázáno praktické řešení zadaného rotoru s pomocí vyvinutého programu spolu s uvedením výsledné průhybové čáry, kritických otáček a tepelných ztrát v ložiscích. V závěru je také provedeno srovnání výsledků pro další přístup stanovení tuhosti ložiska, zvláště pak vliv na kritické otáčky daného rotoru, závěry ze vzájemného porovnání jsou následovně implementovány ve vyvinutém řešiči.

**Keywords**

Rotor system, Transfer matrix method, Bearing stiffness, Critical speed, Hertz's elastic contact theory, Heat loss

**Klíčová slova**

Rotorové soustavy, Metoda přenosových matic, Tuhost ložisek, Kritické otáčky, Teorie Hertzova kontaktního tlaku, Tepelné ztráty

## Rozšířený abstrakt

Tato diplomová práce se zabývá modelováním rotorových soustav pomocí přenosových matic, s uvažením vlivu magnetického tahu, charakteristického pro elektrické stroje. Dalším významným uvažovaným vstupním parametrem je hodnota tuhosti ložiskových podpor řešeného rotoru. Výsledky statické analýzy v podobě silových reakcí v ložiskových podporách mohou být dále využity pro odhad tepelných ztrát indukovaných v ložiscích hřídele rotoru.

Metoda přenosových matic je populární metoda pro řešení soustav diferenciálních rovnic popisující systémy sériově řazených prvků. Hřídel v elektrické stroji skládající se ze segmentů o různých průřezích, nesoucí součásti, jako například ozubená kola, či řemenice, a podepřené ložisky o určité tuhosti určitě může být chápán jako systém sériově řazených. Metoda přenosových matic umožňuje časově efektivní řešení průhybu hřídele, stanovení silových reakcí v pružných podporách a výpočet kritických otáček daného rotoru.

Tuhost ložiskových podpor, je významným parametrem, který ovlivňuje dynamické vlastnosti rotorové soustavy. V této práci je nastíněn postup odhadu tuhosti valivého ložiska na základě teorie Hertzova kontaktního tlaku, kdy lze stanovit tuhost kontaktu valivkého elementu ložiska s s oběžnými dráhami vnějšího a vnitřního prstence ložiska, a to z geometrických rozměrů daného ložiska.

Třecí ztráty generované v ložisku lze odhadnout na základě známého radiálního zatížení ložiska a na provozních otáčkách. Ve třecích ztrátách lze zohlednit také vliv maziva ložiska, případně těsnění ložiska.

Na základě teoretických poznatků výše zmíněných problematik, byl navržen softwarový řešič, vyvinutý pomocí výpočtového prostředí MATLAB. Navržený program umožňuje statickou a dynamickou analýzu zadané rotorové soustavy, pomocí algoritmu přenosových matic. Výsledky silových reakcí lze v tomtéž řešiči použít pro stanovení tepelných ztrát ve vybraném ložisku daného rotoru.

Navržený řešič byl použit pro dvě analýzy rotorové soustavy. V prvním případě byla tuhost podpor stanovena na základě zmíněné Hertzovy teorie kontaktního tlaku, v druhém případě byly tuhosti ložiskových podpor stanoveny na základě vztahu odvozeného z předpokladu rozložení radiálního zatížení mezi více valivých elementů ložiska. Na základě srovnání dosažených výsledků byla navržena jistá úprava v ovládání výpočtu v daném programu, a to zejména s ohledem na kritické otáčky rotoru. Výpočet se musí skládat dílčích iteračních výpočtů v případě, že tuhost ložiskových podpor není na počátku blíže stanovena.



**Bibliographic citation**

TOBIÁŠ, J. *Analysis of transfer matrix method using for calculation of electrical machines rotor with influence of magnetic pull*. Brno: Brno University of Technology, Faculty of Mechanical Engineering, 2022. 62 s. Supervisor Assoc. Prof. Radek Vlach, Ph.D.



I declare honestly, that presented mater thesis has been completed solely by myself under the supervision of Assoc. Prof. Radek Vlach, Ph.D., and that all resources used in this thesis have been properly cited.

Bc. Jan Tobiáš



I wish to thank to Assoc. Prof. Radek Vlach, Ph.D. for guidance during the completing of the topic of this thesis. I would like to appreciate to Ing. Petr Lošák, Ph.D. for his willingness to provide me precious advice in the practical task of this thesis. The biggest gratitude I would like to express to my family for the moral and material support during the whole period of my university studies.



# Contents

<b>1</b>	<b>Introduction</b>	<b>3</b>
1.1	Motivation . . . . .	3
1.2	Problem definition . . . . .	3
1.3	Objectives settings . . . . .	3
<b>2</b>	<b>Beam computations</b>	<b>4</b>
2.1	Castigliano's Method . . . . .	4
2.2	Deflection curve . . . . .	4
2.3	Method of initial parameters . . . . .	5
2.4	Transfer matrix method . . . . .	6
2.4.1	Establish of transfer matrix . . . . .	6
2.4.2	Computational algorithm . . . . .	7
2.4.3	Loading incorporation . . . . .	8
2.4.4	Bearing reactions . . . . .	10
2.4.5	Boundary conditions . . . . .	10
2.4.6	Dynamic response . . . . .	11
<b>3</b>	<b>Magnetic pull</b>	<b>14</b>
3.1	Eccentricity model . . . . .	14
3.2	Force and stiffness model . . . . .	15
3.3	Simplification assumptions . . . . .	15
3.4	Transfer matrix model . . . . .	16
<b>4</b>	<b>Rolling-Element Bearings</b>	<b>17</b>
4.1	Bearing types . . . . .	17
4.1.1	Ball Bearings . . . . .	18
4.1.2	Roller Bearings . . . . .	19
<b>5</b>	<b>Bearing stiffness</b>	<b>20</b>
5.1	Hertz's contact . . . . .	20
5.1.1	Elliptical contacts . . . . .	20
5.1.2	Rectangular contact . . . . .	23
5.1.3	Material properties . . . . .	24
5.1.4	Stiffness estimation . . . . .	24
5.2	Preloaded bearing . . . . .	25
<b>6</b>	<b>Power losses</b>	<b>27</b>
6.1	Loading friction . . . . .	27
6.2	Lubricant friction . . . . .	28
6.3	Sealing friction . . . . .	28
<b>7</b>	<b>Software interface</b>	<b>30</b>
7.1	MATLAB . . . . .	30
7.2	Python . . . . .	30
7.3	C++ . . . . .	30

<b>8</b>	<b>Rotor shaft solver</b>	<b>31</b>
8.1	Input parameters . . . . .	33
8.1.1	Elements definition . . . . .	33
8.1.2	Bearing parameters . . . . .	35
8.1.3	Material and Speed Range . . . . .	36
8.1.4	Boundary conditions . . . . .	36
8.2	Shaft visualize . . . . .	37
8.3	Shaft Results . . . . .	37
8.4	Bearing Results . . . . .	37
8.5	Project control . . . . .	39
8.5.1	Computation . . . . .	39
8.5.2	Data save . . . . .	40
8.6	Warning dialogues . . . . .	43
8.7	Software installation . . . . .	45
<b>9</b>	<b>Application</b>	<b>46</b>
9.1	Solved rotor . . . . .	46
9.1.1	Bearing stiffness calculation . . . . .	48
9.1.2	Analysis setting . . . . .	51
9.1.3	Obtained results . . . . .	52
9.2	Influence of the bearing stiffness . . . . .	55
9.3	Improved rotor analysis . . . . .	56
9.4	Validation . . . . .	58
9.5	Software improvement . . . . .	59
9.5.1	Illustrative example . . . . .	61
<b>10</b>	<b>Summary</b>	<b>62</b>
<b>11</b>	<b>List of appendix and used software</b>	<b>63</b>

# 1. Introduction

## 1.1. Motivation

Rotary machines are one of the most important elements of industrial devices and rotating shafts are the most critical elements of these machines. The prime role of the shaft is the power transmission, furthermore these shafts are supposed to bear other machine parts like discs, bearings, gears, or rotors, especially in electric motors. There have been developed various methods to analyse the rotary systems. One of these methods is the transfer matrix method. The benefit of this method is the fact it is convenient to model serial systems, which the shaft bearing plenty of other parts is indeed. Such shaft can be split into particular segments. Individual segments can be described by its specific transfer matrix. These matrices can be derived from dynamic equations or can be already found as tabulated results in engineering handbooks. Because of the algorithm principle this method is time efficient for such sort of problems in shaft analysis. In the end it leads to estimate deflection and critical speed of the shaft and force reactions in the rotor bearing. However there exist several factors that influence the result accuracy of the computation compared to the real state. Especially in electric machines it depends on how precisely the magnetic pull arising from the interaction between rotor and stator is modelled. Moreover, it depends how the value of the stiffness of the bearing considered as a spring support is estimated, these factors have consequently an impact to determined deflection and critical speed of the shaft. One more output that can be estimated in the rotor system analysis is heat loss generated in the rotor bearing. This variable is depended on the specific bearing type, its reactions, which gives us a value of the bearing load, and operational rotational speed of the rotor as well.

## 1.2. Problem definition

The problem addressed master thesis is numerical modelling of rotor bearing system. The model should respect the following key factors: magnetic pull, bearing stiffness given by specific type of the bearing chosen by designer, influence of the different approaches to estimate bearing stiffness to critical speed, and bearing reactions consequently affecting generated heat loss in the bearings.

## 1.3. Objectives settings

1. Research in field of mathematical modelling of electric engines rotor bearing system, focused on application of the transfer matrix method.
2. Devise a software solver for simulating rotor bearing system with aim to obtain deformation, critical speed of the rotor shaft and heat loss in the shaft bearings.
3. Implementation of methods for estimating bearing stiffness and heating losses induced in the bearings into the rotor analysis.
4. Affect of bearing stiffness on rotor critical speed and bearing heat loss.
5. Analysis and comparison of obtained results.

## 2. Beam computations

Rotary machine shaft can be modelled in several ways, from the theory of stress-strain analysis it follows that suitable model for rotor shaft is one dimensional beam body. Characteristic property of such model is that it includes three displacements and three rotations as degrees of freedom in the endpoints of the beam body. Therefore, it makes it possible to describe the body in cases when it is subjected to bending load. This chapter is oriented on review of mathematical methods for beam models computations.

### 2.1. Castigliano's Method

The main idea of this method in stress strain analysis theory is to estimate resulting displacement in linear-elastic body systems of the point of causing force. It is defined as partial derivative of strain energy of the entire system with respect to certain causing force. The form for beam bending computation is mentioned below, in formula (2.1). The limitation of this method is that it makes possible to obtain only the displacement  $u_k$  in point of causing force  $F_k$  [1].

$$u_k = \frac{\partial A}{\partial F_k} = \frac{\partial}{\partial F_k} \int_{\gamma} \frac{M_y^2(x) dx}{2EJ_y} = \int_{\gamma} \frac{M_y(x)}{EJ_y} \frac{\partial M_y}{\partial F_k} dx \quad (2.1)$$

### 2.2. Deflection curve

This method is based on solving the differential equation for deflection curve of bended beam, formula (2.2). Compared to the previous method it makes it possible to get the outcome as shape function of the deflection along the whole loaded beam, and not only in the points of certain force loading. The necessity for solving the equation is to introduce boundary conditions which express the beam ending point state variables regarding to the real mounting conditions of the beam [1].

$$EJ_y \cdot w^{ii}(x) = -M_y(x) \quad (2.2)$$

Deformation and internal force effects in arbitrarily point along the beam axes can be described by following state variables:

- $w$  displacement
- $\theta$  slope
- $M$  bending momentum
- $T$  transversal force

Governing equations, which makes is possible to solve the differential equation are [2]:

$$\frac{dw}{dx} = -\theta \qquad \frac{d\theta}{x} = \frac{M}{EJ} \qquad \frac{dM}{x} = T$$

## 2.3. Method of initial parameters

Method of initial parameters is specific way to formulate general solution of differential equation. The basis of this method is to transform boundary problem to initial problem. Integration constants are expressed via function values of state variables in the origin of the coordinate system, which is usually placed in the left side endpoint of the solved beam. It is usual case that the parameters in the origin are unknown, and it is needed to estimate them by transformation from conditions known in other points of the beam system [2].

Significant advantage of this method is the possibility to solve the problems of beams on elastic foundations with discontinuities along the beam span caused by applied forces or segments with different cross section areas [2].

For instance, here will be shown solution of beam subjected to bending caused only by transversal forces, as it is stated in [2].

The problem can be described by the homogeneous differential equation of the fourth order with the solution in the following way.

$$\begin{aligned}
 w^{iv}(x) &= 0 \\
 w^{iii}(x) &= c_1 \\
 w^{ii}(x) &= c_1x + c_2 \\
 w^i(x) &= c_1\frac{x^2}{2} + c_2x + c_3 \\
 w(x) &= c_1\frac{x^3}{6} + c_2\frac{x^2}{2} + c_3x
 \end{aligned} \tag{2.3}$$

The boundary conditions (initial parameters) are:

$$w(0) \quad w^{ii}(0) \quad M(0) = -EJ_y \cdot w^{ii}(0) \quad T(0) = -EJ_y \cdot w^{iii}(0)$$

Estimated integration constants from the initial parameters are:

$$c_1 = \frac{T(0)}{EJ_y} \quad c_2 = \frac{M(0)}{EJ_y} \quad c_3 = w^i(0) \quad c_4 = w(0)$$

By substitution of attained constants to formulas in (2.3) the following system of equations can be obtained.

$$\begin{aligned}
 w(x) &= w(0) + w^i(0) \cdot x - \frac{M(0) \cdot x^2}{2EJ_y} - \frac{T(0) \cdot x^3}{6EJ_y} \\
 w^i(x) &= w^i(0) \cdot x - \frac{M(0) \cdot x}{EJ_y} - \frac{T(0) \cdot x^2}{24EJ_y} \\
 M(x) &= M(0) + T(0) \cdot x \\
 T(x) &= T(0)
 \end{aligned} \tag{2.4}$$

The results achieved in this section will be used later for explanation of principle of the following method.

## 2.4. Transfer matrix method

Transfer matrix method is a matrix form of method of initial parameters. During times it had shown to be extraordinarily effective method for solving differential equations for serial system. The method is characterized by progressive matrix multiplications along a line of the serial system. This step leads to final matrix whose size does not depend on the number of elements in the solved system, which is the significant advantage property of this method in comparison with the finite element method [2], [3].

### 2.4.1. Establish of transfer matrix

The basic idea of the transfer matrix method will be explained on the previous example with bended beam. The system of equations (2.4) can be written in matrix form as follows [2]:

$$\begin{bmatrix} w \\ \theta \\ M \\ T \end{bmatrix}_x = \begin{bmatrix} 1 & x & -\frac{x^2}{2EJ_y} & -\frac{x^3}{6EJ_y} \\ 0 & 1 & -\frac{x}{EJ_y} & -\frac{x^2}{2EJ_y} \\ 0 & 0 & 1 & x \\ 0 & 0 & 0 & 1 \end{bmatrix} \cdot \begin{bmatrix} w \\ \theta \\ M \\ T \end{bmatrix}_0 \quad (2.5)$$

The state variables in the matrix form are gathered in a so-called state vector.

In short form it is denoted [2]:

$$\{w\}_x = [C]_{x,0}^0 \{w\}_0 \quad (2.6)$$

Used notation means:

- $\{w\}_x$  state vector at specific point  $x$  along the axes of the beam body
- $\{w\}_0$  initial state vector given by the values in the origin of the coordinates
- $[C]_{x,0}^0$  linear transformation; transfer matrix for the field on interval  $[0, x]$

The transfer matrix can be derived in general for the problems described by differential equations. The procedure will be shown again with the example of the bended beam. The system of equations (2.3) can be written in matrix form.

$$\begin{bmatrix} w \\ w^i \\ w^{ii} \\ w^{iii} \end{bmatrix}_x = \begin{bmatrix} 1 & x & \frac{x^2}{2} & \frac{x^3}{6} \\ 0 & 1 & x & \frac{x^2}{2} \\ 0 & 0 & 1 & x \\ 0 & 0 & 0 & 1 \end{bmatrix} \cdot \begin{bmatrix} c_4 \\ c_3 \\ c_2 \\ c_1 \end{bmatrix}_0 \quad (2.7)$$

The system can be written in short form.

$$\{w\}'_x = [F]_x \{c\} \quad (2.8)$$

Used notation means:

- $\{w\}'_x$  vector including solution of differential equation  $w^{iv}(x) = 0$
- $\{c\}$  vector of integration constants
- $[F]$  fundamental matrix (Wronskian)

The initial parameters can be formulated in analogous way.

$$\{w\}'_0 = [F]_0\{c\} \quad (2.9)$$

By execution of  $c$  from equation (2.9) and substitution into equation (2.6) it is obtained.

$$\{w\}'_x = [F]_x[F]_0^{-1}\{w\}'_0 \quad (2.10)$$

The vector  $\{w\}'_x$  can be transformed to vector  $\{w\}_x$  by matrix  $[R]$  as follows:

$$\begin{bmatrix} w \\ w^i \\ w^{ii} \\ w^{iii} \end{bmatrix}_x = \begin{bmatrix} 1 & 0 & 0 & 0 \\ 0 & 1 & 0 & 0 \\ 0 & 0 & -EJ_y & 0 \\ 0 & 0 & 0 & -EJ_y \end{bmatrix} \cdot \begin{bmatrix} w \\ w^i \\ w^{ii} \\ w^{iii} \end{bmatrix}_0 \quad (2.11)$$

By execution of  $\{w\}'_x$  from equation (2.11) and substitution into equation (2.10), the state vector can be expressed.

$$\{w\}_x = [R][F]_x[F]_0^{-1}[R]^{-1}\{w\}_0 \quad (2.12)$$

Observed from formula above, general formulation of transfer matrix is:

$$[C] = [R][F]_x[F]_0^{-1}[R]^{-1} \quad (2.13)$$

### 2.4.2. Computational algorithm

The general transfer formula (2.6) can be formulated for several beam segments in row along the beam axis. Total length of the beam body is divided into specific sub-intervals according to the specific elements [3]. For instance, according to the figure below.

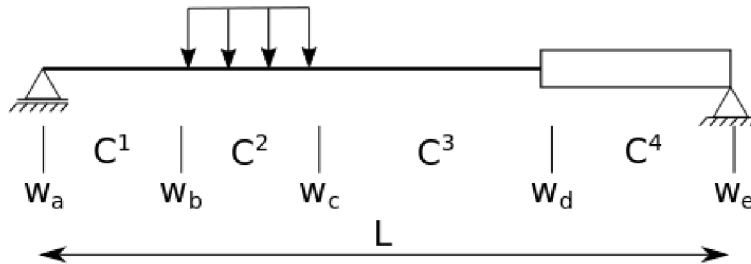


Figure 2.1: Beam with denoted segments [3]

Transfer formulas for each sub-interval are expressed in following forms [3].

$$\begin{aligned}
\{w\}_b &= [C]_{a,b}^1 \{w\}_a \\
\{w\}_c &= [C]_{b,c}^2 \{w\}_b \\
\{w\}_d &= [C]_{c,d}^3 \{w\}_c \\
\{w\}_e &= [C]_{d,e}^4 \{w\}_d
\end{aligned} \tag{2.14}$$

The state vectors  $\{w\}_a, \{w\}_b, \{w\}_c, \{w\}_d$  contain state variables at dividing points. From the equation system above it is obvious that vectors at dividing points can be progressively expressed by the vector from the initial point, that leads to system of equations [3].

$$\begin{aligned}
\{w\}_c &= [C]_{a,b}^2 [C]_{a,b}^1 \{w\}_a \\
\{w\}_d &= [C]_{d,c}^3 [C]_{c,b}^2 [C]_{b,a}^1 \{w\}_a \\
\{w\}_e &= [C]_{e,d}^4 [C]_{d,c}^3 [C]_{c,b}^2 [C]_{b,a}^1 \{w\}_a
\end{aligned} \tag{2.15}$$

The equations have shown other way to obtain the state vector at any point by multiplication of transfer matrices, from endpoint on the left side up to the chosen point, with the initial state vector in the left endpoint of the beam. The matrix coming from the multiplication of matrices of all elements is called global transfer matrix [2], [3].

Computer computation is based on two major steps, the first one is to establish the global transfer matrix of the system. After that boundary conditions are applied to global matrix, thus initial state vector becomes known. Further it follows another multiplication along the system according to the (2.14) and (2.15) which permits to print out the state variables responses of the entire system along the system elements [3].

### 2.4.3. Loading incorporation

Influence of such external occurrences as springs, lumped masses, concentrated transverse forces or distributed load along the beam axes is expressed by involving particular solution of certain differential equation in the following way [2]:

$$\{w\}_x = [C]_{x,0}^0 \{w\} + \{w_p\}_x \tag{2.16}$$

The second term  $\{w_p\}_x$ , which denotes particular solution of differential equation in general, corresponds to impulse response of the system to change of state variables in solved field. It is usual to incorporate the loading terms directly in the transfer matrix with the aim to make the computations more convenient. This is done by defining extended state vector and extended state matrix through mathematical identity  $1 = 1$ , as it follows [2].

$$\begin{bmatrix} w \\ \theta \\ M \\ T \\ 1 \end{bmatrix}_x = \begin{bmatrix} 1 & x & -\frac{x^2}{2EJ_y} & -\frac{x^3}{6EJ_y} & F_w \\ 0 & 1 & -\frac{x}{EJ_y} & -\frac{x^2}{2EJ_y} & F_\theta \\ 0 & 0 & 1 & x & F_M \\ 0 & 0 & 0 & 1 & F_T \\ 0 & 0 & 0 & 0 & 1 \end{bmatrix} \cdot \begin{bmatrix} w \\ \theta \\ M \\ T \\ 1 \end{bmatrix}_0 \tag{2.17}$$

As it has been mentioned above using the shown extension via the last column in extended matrix helps to add influence of external causing load into computation. Through that idea can be expressed the effect of the beam's mass distributed along its axis. Specific extended form of the matrices describing the beam segments are stated in appendix of this thesis, Transfer matrices.

Next, it will be explained derivation of the matrices for spring supports and concentrated transverse force. These two cases have in common the expression of step change of the state variables in field of the beam body, matrices for these cases are referred also as point matrices.

Suppose concentrated transverse force at point  $j$  of the solved beam body. Consider infinitesimally short spanning element around the point  $j$ . As it illustrates the figure 2.2 below [3].

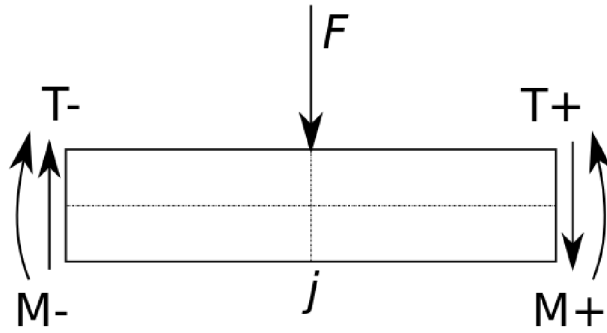


Figure 2.2: Beam segment at point  $j$  [3]

Deflection and slope are continuous across  $j$ . Summation of momentum of point  $j$  implies that bending momentum is also continuous. However, equilibrium of the vertical forces shows the change of shear force between left and right side with the magnitude corresponding to value of the subjecting transverse force  $F$ . All of that can be expressed by equation for specific point  $j$  [3]:

$$\begin{bmatrix} w \\ \theta \\ M \\ T \\ 1 \end{bmatrix}_j = \begin{bmatrix} w \\ \theta \\ M \\ T \\ 1 \end{bmatrix}_j + \begin{bmatrix} 0 \\ 0 \\ 0 \\ -F \\ 1 \end{bmatrix}_j \quad (2.18)$$

The equilibrium can be written in matrix form, where the matrix is transfer matrix for step change of transverse force at certain point of the beam [3]:

$$\begin{bmatrix} w \\ \theta \\ M \\ T \\ 1 \end{bmatrix}_j = \begin{bmatrix} 1 & 0 & 0 & 0 & 0 \\ 0 & 1 & 0 & 0 & 0 \\ 0 & 0 & 1 & 0 & 0 \\ 0 & 0 & 0 & 1 & -F \\ 0 & 0 & 0 & 0 & 1 \end{bmatrix} \cdot \begin{bmatrix} w \\ \theta \\ M \\ T \\ 1 \end{bmatrix}_j \quad (2.19)$$

The idea for derivation of spring support matrix is the same with such distinction, that the force at point  $j$  is given by spring stiffness  $k$  and displacement  $w_j$  at point  $j$ . Transfer matrix formulation for such case is [3].

$$\begin{bmatrix} w \\ \theta \\ M \\ T \\ 1 \end{bmatrix}_j = \begin{bmatrix} 1 & 0 & 0 & 0 & 0 \\ 0 & 1 & 0 & 0 & 0 \\ 0 & 0 & 1 & 0 & 0 \\ 0 & 0 & 0 & 1 & kw_j \\ 0 & 0 & 0 & 0 & 1 \end{bmatrix} \cdot \begin{bmatrix} w \\ \theta \\ M \\ T \\ 1 \end{bmatrix}_j = \begin{bmatrix} 1 & 0 & 0 & 0 & 0 \\ 0 & 1 & 0 & 0 & 0 \\ 0 & 0 & 1 & 0 & 0 \\ k & 0 & 0 & 1 & 0 \\ 0 & 0 & 0 & 0 & 1 \end{bmatrix} \cdot \begin{bmatrix} w \\ \theta \\ M \\ T \\ 1 \end{bmatrix}_j \quad (2.20)$$

Spring support element can be used in the system as model of bearing with specific the stiffness. The ways to estimate the bearing stiffness will be discussed in another chapter.

#### 2.4.4. Bearing reactions

One of the sought outcomes of the rotor system analysis are bearing reaction forces. As explained in the previous section, the transverse forces or spring supports cause the step change of the transverse force state variable. There exists following mathematical expression of the step change around the spring support:

$$\begin{bmatrix} w \\ \theta \\ M \\ R_j \\ 1 \end{bmatrix}_b = \begin{bmatrix} 1 & 0 & 0 & 0 & 0 \\ 0 & 1 & 0 & 0 & 0 \\ 0 & 0 & 1 & 0 & 0 \\ k & 0 & 0 & 1 & 0 \\ 0 & 0 & 0 & 0 & 1 \end{bmatrix}_{b,a} \cdot \begin{bmatrix} w \\ \theta \\ M \\ T \\ 1 \end{bmatrix}_a - \begin{bmatrix} w \\ \theta \\ M \\ T \\ 1 \end{bmatrix}_a \quad (2.21)$$

The state vector at point  $a$  contains the values of the state variables on the one side of the spring support, by the multiplication with the spring support transfer matrix it is obtained the state variables on the other side of the support. By the subtraction of these two vectors, the vector with the bearing force reaction  $R_j$  is obtained.

#### 2.4.5. Boundary conditions

As it has been declared, boundary conditions are necessary to gain the initial state vector. Here will be given an insight into the process to apply prescribed boundary conditions into computation. Consider bended beam described in general by transfer formula (2.6) expressing relation between state vectors at the beginning  $x = 0$  and at the end  $x = L$  of the beam. Further, suppose the global transfer matrix has been already attained [4].

$$\begin{bmatrix} w \\ \theta \\ M \\ T \\ 1 \end{bmatrix}_L = \begin{bmatrix} C_{11} & C_{12} & C_{13} & C_{14} & C_{15} \\ C_{21} & C_{22} & C_{23} & C_{24} & C_{25} \\ C_{31} & C_{32} & C_{33} & C_{34} & C_{35} \\ C_{41} & C_{42} & C_{43} & C_{44} & C_{45} \\ C_{51} & C_{52} & C_{53} & C_{54} & C_{55} \end{bmatrix} \cdot \begin{bmatrix} w \\ \theta \\ M \\ T \\ 1 \end{bmatrix}_0 \quad (2.22)$$

For bended beam four boundary conditions are required through prescribed values of state variable in the endpoints of the beam. These values are substituted to corresponding positions in the initial and the final state vectors of the beam in transfer formula (2.22), [2], [4].

For instance, suppose beam founded on spring supports with free end points, corresponding boundary conditions are:

- for  $x = 0$ :  $M(0) = 0$ ;  $T(0) = 0$
- for  $x = L$ :  $M(L) = 0$ ;  $T(L) = 0$

Implementing these conditions to formula (2.22) leads to elimination of columns matching to positions of zero values in initial state vector and rows matching to unknown values in the endpoint state vector, last row can be omitted as well[4].

$$\begin{bmatrix} w \\ \theta \\ M = 0 \\ T = 0 \\ 1 \end{bmatrix}_L = \begin{bmatrix} \rightarrow & \rightarrow & \rightarrow & \rightarrow & \rightarrow \\ \rightarrow & \rightarrow & \rightarrow & \rightarrow & \rightarrow \\ C_{31} & C_{32} & \rightarrow & \rightarrow & C_{35} \\ C_{41} & C_{42} & \rightarrow & \rightarrow & C_{45} \\ \rightarrow & \rightarrow & \rightarrow & \rightarrow & \rightarrow \end{bmatrix} \cdot \begin{bmatrix} w \\ \theta \\ M = 0 \\ T = 0 \\ 1 \end{bmatrix}_0 \quad (2.23)$$

Gained reduced system of equations make solving of remaining initial state variables possible. Such achieved initial state vector can be used in following computation to print out the state variables response along the beam structure as it explains the previous section about the computational algorithm.

## 2.4.6. Dynamic response

Previous sections have been focused on solving of static problems. However, also dynamic problems including the inertia of the acceleration of the structural mass effects has to be taken into account. The responses of the structure in dynamic problems are so-called natural modes, which are characteristic deformation shapes of the structure body, that occurs under the action of initial displacement and velocity conditions. Each natural mode is related to certain natural frequency, therefore, to obtain only one of these two information is enough to predict the dynamic response of the structure. Relatively logical approach to get the natural frequency of the beam structure provides transfer matrix methodology [3].

Suppose bended beam, free motion is governed by the following equation [3]:

$$\frac{\partial^2}{\partial x^2} \left( EI \frac{\partial^2 w}{\partial x^2} \right) = -\rho \frac{\partial^2 w}{\partial t^2} \quad (2.24)$$

Additional governing equation to solve the problem are [3]:

$$\frac{dw}{dx} = -\theta \quad \frac{d\theta}{dx} = \frac{M}{EJ} \quad \frac{dM}{dx} = T \quad \frac{dT}{dx} = -\rho\omega^2 w \quad (2.25)$$

The procedure to solve the equations above can be done in the analogous way as the static problem. For serial segmented beam structures can be composed global transfer matrix by progressive multiplication of the transfer matrices of each segment of the structure. These matrices are stated in the appendix of this thesis, Transfer matrices.

Consider bended beam with identical boundary condition as in the static problem above.

- for  $x = 0$ :  $M(0) = 0$ ;  $T(0) = 0$
- for  $x = L$ :  $M(L) = 0$ ;  $T(L) = 0$

Transfer form for the entire system with its global transfer matrix will be obtained, as it has been explained in the case with the static problem above. In general, it can be written as follows [4].

$$\begin{bmatrix} w \\ \theta \\ M \\ T \end{bmatrix}_L = \begin{bmatrix} U_{11} & U_{12} & U_{13} & U_{14} \\ U_{21} & U_{22} & U_{23} & U_{24} \\ U_{31} & U_{32} & U_{33} & U_{34} \\ U_{41} & U_{42} & U_{43} & U_{44} \end{bmatrix} \cdot \begin{bmatrix} w \\ \theta \\ M \\ T \end{bmatrix}_0 \quad (2.26)$$

The boundary conditions will be applied, and reduced system of equations will be obtained [3], [4]:

$$\begin{bmatrix} w \\ \theta \\ M = 0 \\ T = 0 \end{bmatrix}_L = \begin{bmatrix} \rightarrow & \rightarrow & \rightarrow & \rightarrow \\ \rightarrow & \rightarrow & \rightarrow & \rightarrow \\ U_{31} & U_{32} & \rightarrow & \rightarrow \\ U_{41} & U_{42} & \rightarrow & \rightarrow \end{bmatrix} \cdot \begin{bmatrix} w \\ \theta \\ M = 0 \\ T = 0 \end{bmatrix}_0 \quad (2.27)$$

In accordance with the formulas from the appendix (Transfer matrices), the terms of the matrix depend through the coefficient  $\gamma$  on the angular velocity (rotation)  $\omega$ . The distinction compared to the static problem is, the original system of equations is in dimension  $4 \times 4$ , not  $5 \times 5$ . This causes the system indeterminate since five variables are unknown: the state variables and the rotational speed  $\omega$  [3], [4].

The reduced system of equations is called homogeneous, nontrivial solution of such system exists if determinant of the system matrix is zero. Because the determinant is a function of the unknown rotation  $\omega$ , the value of the determinant can be tracked on dependency of the rotation  $\omega$ . The values of  $\omega$  corresponding to zero determinant are desired natural frequencies  $\Omega$  of the solved beam structure [3].

## Use of bisection method

Tracking the root of the relation between the angular velocity and the determinant of the reduced system can be solved numerically, appropriate method for such problems is bisection method [6].

The method is based on Bolzano's theorem for continuous functions [5], [6].

If it holds for a function  $f(x)$  on certain interval  $[a, b]$  that  $f(a) \cdot f(b) < 0$ , then there must exist  $c \in (a, b)$  for which  $f(c) = 0$ , [6].

The bisection method looks to find an approximation of the root of the function  $f(x)$ . The accuracy of the approximation is given by tolerance  $\epsilon$  set for the algorithm. The algorithm as is stated in [5],[6], follows these steps:

1. by tracking the function values with respect to condition in Bolzano's theorem, values  $a$  and  $b$  are chosen
2. **interval halving:** midpoint  $c$  as an arithmetic mean between  $a$  and  $b$  is estimated
3. function  $f$  is evaluated for  $c$
4. if  $f(c) \neq 0$ , the sign of  $f(c)$  is checked
  - if  $f(c)$  has the same sign as  $f(a)$ ,  $b$  is replaced by  $c$
  - if  $f(c)$  has the same sign as  $f(b)$ ,  $a$  is replaced by  $c$
5. calculation continues again from step 2., new values of  $a$  or  $b$  are recalculated

The tolerance  $\epsilon$  is the absolute value of the difference  $|c - x|$  between value of  $c$  and the actual root  $x$ . For the convergence within an absolute error tolerance  $\epsilon$  it is needed to meet the condition [5], [6]:

$$|c - x| \leq \epsilon \quad (2.28)$$

The iterative loop for certain interval  $[a, b]$  lasts until the recalculated values of  $a_n$  and  $b_n$  in  $n^{th}$  iteration meet the condition [6]:

$$\frac{b_n - a_n}{2} = \epsilon = |c_n - x| \quad (2.29)$$

Hence, the value of  $c_n$ , given as an arithmetic mean of the  $a_n$  and  $b_n$ , can be considered as an approximation of the root  $x$  of the tracked function within the certain tolerance  $\epsilon$  [5], [6].

The application of the bisection method in the calculations of the natural modes in rotor shaft analysis is as it follows:

- the range of the rotation speed of the solved shaft is given
- interval step of the rage is given
- determinant of the reduced transfer matrix (2.27) is tracked depending on the given rotation speed range, in accordance with the algorithm stated above

Numerical tracking of the determinant is not giving continuous waveform of the function values. Therefore, the bisection, especially the evaluation of the  $c$  value, is done through a linear approximation of the bounds  $a_n$  and  $b_n$  in current  $n^{th}$  iteration of the interval halving.

Since the bisection method is linear convergence rate, with the constant  $m = \frac{1}{2}$ , it needs at least  $k$  iterations to get  $2^{-k}$  tolerance. In practical engineering tasks the usual tolerance  $\epsilon$  is two orders smaller than the given interval step. Therefore, seven steps of halving for one initial intervals are processed, since  $2^{-7} = \frac{1}{128}$  and  $\frac{1}{128} < \frac{1}{100}$  [7].

### 3. Magnetic pull

This chapter is focused on brief explanation of magnetic pull, what does it mean, where does it arise from and what is an optimal method to model this phenomenon in electric machines.

Rotor electric machines are composed from two basic parts, rotor, and stator. Between these parts, there is an air gap in which magnetic field operates and consequently induces electromagnetic forces. These forces should ideally cancel out. However, thickness of the air gap is not constant along the rotor and stator due to eccentricity caused by factors like manufacturing imperfections resulting in deviations from ideal cylindrical shape of considered parts. This leads to force interaction between rotor and stator called unbalanced magnetic pull (UMP). This phenomenon is unavoidable in electric machines, therefore it is needed to be taken into account in rotor system modelling. The UMP acts in radial and tangential direction, but the radial component effect is usually larger, therefore the UMP is modelled as loading in radial direction of the rotor shaft [8].

#### 3.1. Eccentricity model

The figure below shows concepts of considered mutual rotor and stator eccentricity. Two coordinate system are deemed, for stator ( $x_1 - y_1$ ) and rotor ( $x_2 - y_2$ ). Static eccentricity  $e_{st}$  and direction angle  $\theta_{st}$  are defined from transition between these two coordinate systems. Dynamic eccentricity  $e_{dy}$  and direction angle  $\theta_{dy}$  are defined in rotor reference coordinate system derived from rotor whirling motion. Then mixed eccentricity can be defined [9], [10]:

$$e_{mix}(t) = \sqrt{(e_{st}\cos\theta_{st} + e_{dy}(t)\cos(\theta_{dy}(t)))^2 + (e_{st}\sin\theta_{st} + e_{dy}(t)\sin(\theta_{dy}(t)))^2} \quad (3.1)$$

The reason, to observe the eccentricity in time dependency, is to express the air gap in the following computations [10].

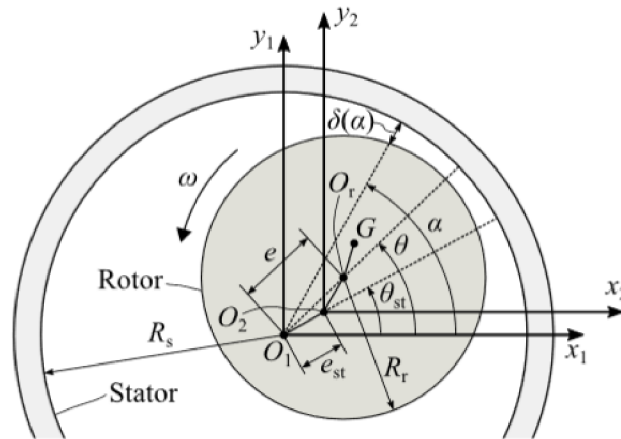


Figure 3.1: Rotor eccentricity scheme [11]

## 3.2. Force and stiffness model

The force of unbalanced magnetic pull can be computed by integration of Maxwell stress tensor in the air gap between rotor and stator. Therefore, it requires to estimate magnetic flux density distribution in the air gap. This can be obtained in terms of air-gap permeance harmonics and surface magnetomotive force harmonics as it follows [9], [10].

$$B_{\delta}(\alpha, t) = \mu_0 \frac{F(\alpha, t)}{\delta(\alpha, t)} = \Lambda(\alpha, t) F(\alpha, t) \quad (3.2)$$

Here,  $\alpha$  denotes location of interested air gap on rotor surface,  $\delta(\alpha, t)$  means the air gap,  $\Lambda(\alpha, t)$  denotes air-gap permeance and  $F(\alpha, t)$  means total magnetomotive force. The UMP forces can be finally calculated as it follows [10].

$$\begin{aligned} F_x &= \int_0^{2\pi} \frac{B_{\delta}(\alpha, t)}{2\mu_0} \cdot r \cdot l_{st} \cdot \cos(\alpha) d\alpha \\ F_y &= \int_0^{2\pi} \frac{B_{\delta}(\alpha, t)}{2\mu_0} \cdot r \cdot l_{st} \cdot \sin(\alpha) d\alpha \end{aligned} \quad (3.3)$$

Here  $r$  is air gap radius and  $l_{st}$  is length of the stator stack.

Obtained UMP force can be used to define magnetic pull stiffness linearized around the static eccentricity  $(x_{st}, y_{st})$  as it follows [9], [10].

$$C_{m,x} \approx \left[ \frac{dF_x}{dx} \right]_{x=x_{st}} \quad C_{m,y} \approx \left[ \frac{dF_y}{dy} \right]_{y=y_{st}} \quad (3.4)$$

## 3.3. Simplification assumptions

The analytical model above has, however, limitations related to the accuracy. The model is established within following simplifications [9]:

- No effect of variation in slip, slot opening, magnetic saturation and flux leakages considered [9]
- Value of mixed eccentricity is static at instantaneous time [9]

Therefore, to overcome mentioned limitations, the usual process is to realize more detailed finite element analysis simulations of the specific magnetic field to achieve results of the mentioned variables with aim to estimate causing forces and eccentricity values for UMP stiffness as precise as possible regarding the specific circumstances [10].

### 3.4. Transfer matrix model

From above stated the model of magnetic pull stated above, resulting in stiffness estimation, that magnetic pull can be taken into account also in numerical model of rotor shafts based on transfer matrix method. The appropriate element type seems to be spring support, however, there are few differences related to the element considered as the one with the magnetic pull effect [4].

First, the stiffness deemed as the magnetic pull is included with negative sign. Briefly, the larger the eccentricity is, the bigger the air gap is, consequently the arising magnetic forces are weaker. That is opposite compared to common mechanical spring model, where the arising force in the spring is growing proportionally with the spring deflection.

Second, it is inappropriate to deem the element with magnetic pull as zero length element. Thus, the approach in such cases is to divide the magnetic pull element into separate shaft type elements and spring support elements with negative value of stiffness in the transfer matrix [4]. However, more appropriate is to discretise the element into more than just two shaft elements with one spring between. The element with the length  $L$  is usually divided internal in the transfer matrix algorithm into  $n$  elements with  $L/n$  length and  $n - 1$  springs are placed between the elements with stiffness  $C_m/n - 1$ .

Exact form of the transfer matrices for magnetic pull elements are stated in the appendix Transfer matrices.

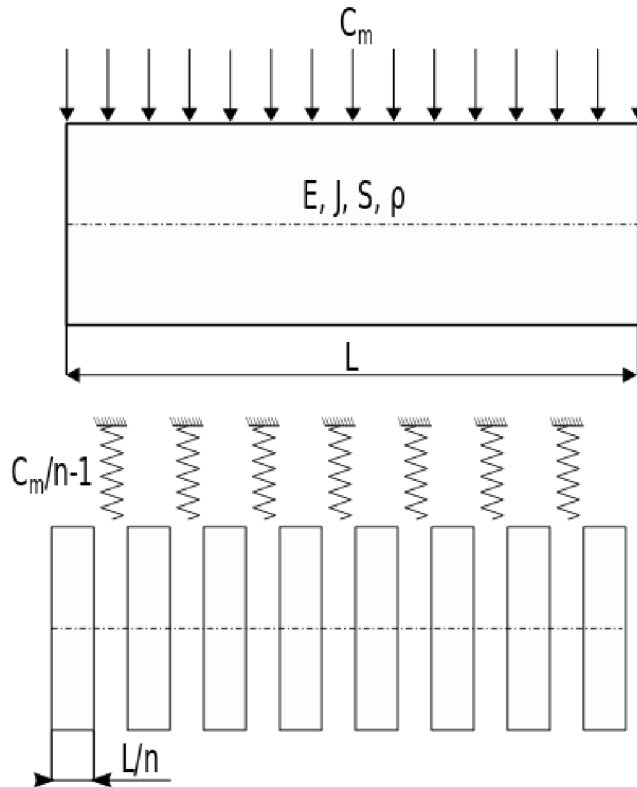


Figure 3.2: Magnetic pull element division scheme

# 4. Rolling-Element Bearings

This chapter considers rolling-element bearings and briefly introduces common types of rolling-element bearing.

## 4.1. Bearing types

There can be considered two basic types of rolling-element bearings, ball bearing and roller bearing. The stated bearing types differs from each other based on the shape of the contact area, the ball bearing has an elliptical contact area, whereas the roller bearing has a rectangular shape of the contact area. The figure 4.1 shows the descriptive pictures of specific bearing types.

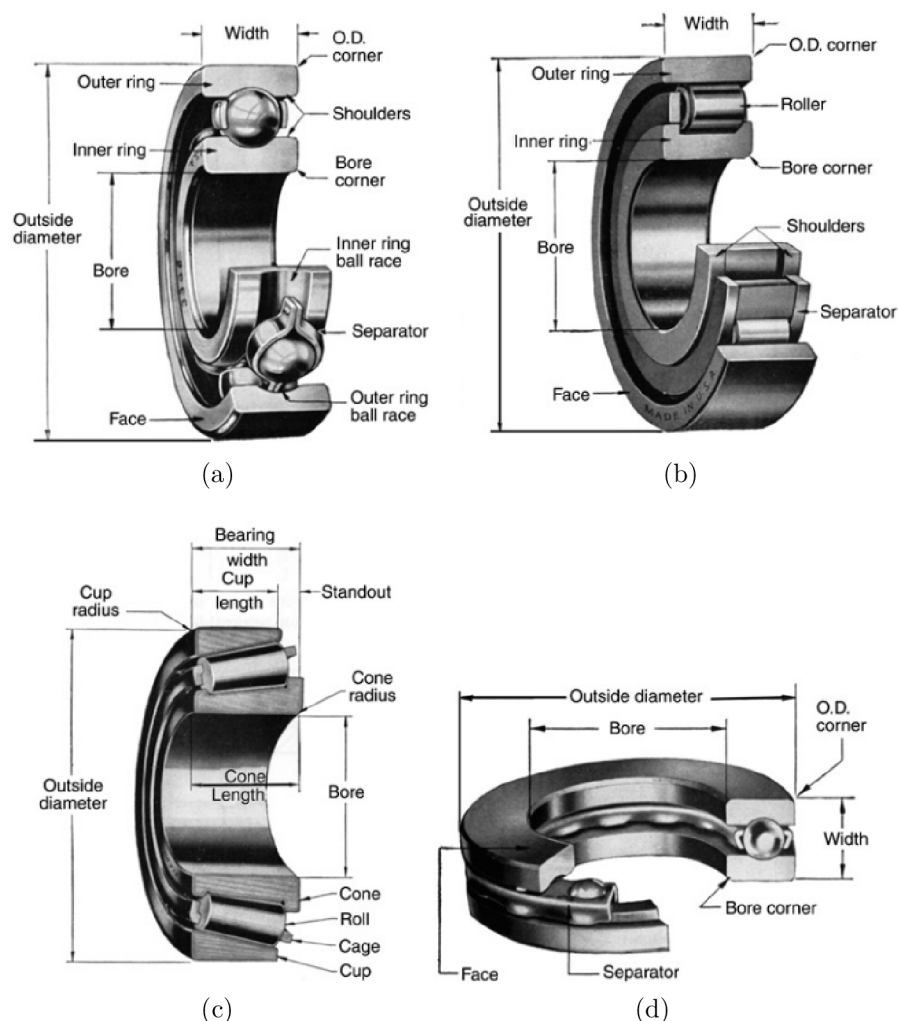


Figure 4.1: Description of the most common rolling-element bearing types [13], (a) Ball bearing, (b) Cylindrical roller bearing, (c) Tapered roller bearing, (d) Thrust ball bearing

As it illustrated the figure 4.1, rolling-element bearings are assembled from several parts: an **inner race**, an **outer race**, a set of balls, or rollers, and cage, or separators. The

cage and separators maintain even spacing between the rolling elements. Full-complement bearings are cage-less, and the annulus is packed with the maximum number of rolling elements. Such type of bearing disposes higher load carrying capacity but lower speed limits compared to cage equipped bearings. Tapered-roller bearings are an assembly of a cup, a cone, a set of tapered roller, and a cage [12].

### 4.1.1. Ball Bearings

The ball bearings are used in greater quantity than any other types of rolling-element. Such type is suitable in application with primarily radial load and some thrust load present. The ability to carry the thrust load can be expressed by the parameter called contact angle [12].

#### Contact angle

The figure 9.4 of the ball bearing cross section depicts the meaning of the contact angle. It is defined as the angle made by line through the points where the ball element touches both inner, and outer raceways and a plane perpendicular to the bearing axis of rotation [12]. The figure implies, the higher contact angle is, the higher is the capacity of the bearing to carry the thrust load.

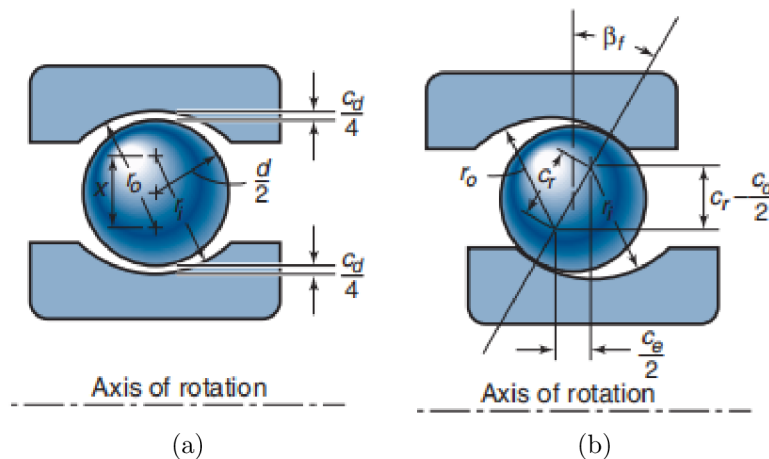


Figure 4.2: Illustration of the bearing contact angle [12], (a) Unloaded ball bearing cross section, (b) Loaded ball bearing cross section with the contact angle

**Deep-groove ball bearing** is the essential type of ball bearing. This kind of ball bearing is not recommended for applications with thrust load, since the contact angle varies from  $0^\circ$  to approximately  $5^\circ$ , because of the radial clearance and an axial play between the raceways and the rollers [12]. As it shows the figure 4.2.

**Angular-contact ball bearings** are designed to carry a heavy thrust load in one direction. It has a two-shouldered ball groove in one raceway and single-shouldered ball groove in the other raceway, as it depicts the figure 4.3. The typical values of the contact angle vary from  $15^\circ$  up to  $40^\circ$  [12]. The angular contact ball bearings are usually mounted in duplex pairs either back-to-back, or face-to-face position. Such case requires the preload so that both bearings are clamped together. The preloaded bearings provides stiffer shaft support and prevent the bearings from skidding at light loads [12].

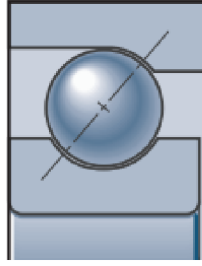


Figure 4.3: Angular-contact ball bearing, cross section detail [12]

**Self-aligning bearings** have an outer race, or inner race ball path in spherical shape, so that it accepts some levels of misalignment [12].

**Thrust ball bearings** have the contact angle  $90^\circ$ , therefore they are applicable exclusively for machinery with vertically oriented shafts [12].

#### 4.1.2. Roller Bearings

Roller bearings are employed for higher loads than can be accommodated with ball bearing. There can be also defined the contact angle in analogous way as for the ball bearings, as it shows the figure 4.4 below [12].

**Cylindrical roller bearings** provide purely radial load support (since the contact angle is zero) with high carrying-load capacity and as well as high speed capability, exceeding spherical, or tapered roller bearings [12].

**Spherical roller bearings** are made either single, or double row design. They combine extremely high radial load capacity with modest thrust-load carrying capacity and have an excellent tolerance to misalignment [12].

**Tapered roller bearings** use rollers in the shape of truncated cones. The radial load capacity is comparable to that of a cylindrical roller bearing with the same size. The contact angle is in range from  $10^\circ$  to  $16^\circ$ , but also steeper contact angle of  $30^\circ$  can be used to increase the thrust load capacity. However, the tapered-roller bearing cannot accept pure radial load and since the assembly is separable, they are usually mounted in pairs, like the angular-contact ball bearing, to improve ability to transfer bidirectional axial load [12], [13].

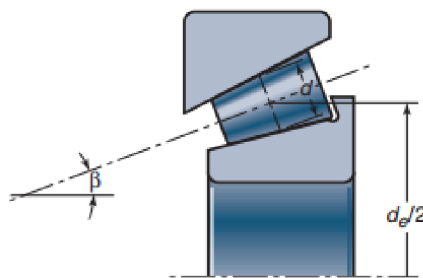


Figure 4.4: Cross section scheme of tapered roller bearing with marked contact angle [12]

# 5. Bearing stiffness

Numerical modelling of bearing is getting more complex nowadays, computations are often made through advanced analysis tools like FEM simulation etc. Such approaches help to develop the knowledge about the problematic of the roller-element bearings. However, there is still need to have useful analytical methods, which can be easily applied by designers in practical task in machine designing. This chapter gives an insight to available approach to estimate a contact stiffness of rolling elements with the ring raceways based on the the bearing geometry [12].

## 5.1. Hertz's contact

The idea to estimate the contact stiffness arises from general load deflection relationship [12]:

$$w_z = K_j \delta^j \quad (5.1)$$

Here,  $K_j$  means bearing rolling element contact stiffness,  $\delta$  means displacement under the causing load in the contact point of the bearing rolling elements. There are two significant types of contact conjunction in the bearings, elliptical for ball bearing or rectangular for roller bearing. These two cases are distinguished via value of  $j$ , for ball bearing it is  $j = 3/2$ , for roller bearing it is  $j = 1$  [12]. The stiffness  $K_j$  for certain contact type can be determined from the bearing geometry, based on the Hertz's elastic contact theory, which will be, for both cases, described in following sections. The method is adopted from the publication [12]. For Hertz's contact theory following factors have to be assumed [14]:

1. The contact body is an isotropic linear elastic material, which obeys Hooke's law and is in a small deformation state.
2. The length  $a$  of the contact area is much smaller than the radius  $R$  of curvature of the surface of the object, that is,  $a \ll R$ .
3. The contact surface is smooth and continuous, and there is no friction.
4. Since  $a \ll R$ , every object can be regarded as an elastic half space.

### 5.1.1. Elliptical contacts

Formula for ball bearing contact stiffness is:

$$K_{1.5} = \pi k_e E' \left( \frac{2\mathcal{E}R}{9\mathcal{F}} \right)^{1/3} \quad (5.2)$$

Used notation means:

- $k_e$       ellipticity parameter
- $E'$       effective module of elasticity
- $R$       curvature sum
- $\mathcal{E}, \mathcal{F}$     elliptic integrals

## Ball bearing geometry

Figure 5.1 depicts cross section of ball bearing geometry. These bearing dimensions are marked: Outer bearing diameter  $d_a$ , inner bearing diameter  $d_b$ , bearing width  $b_w$ .

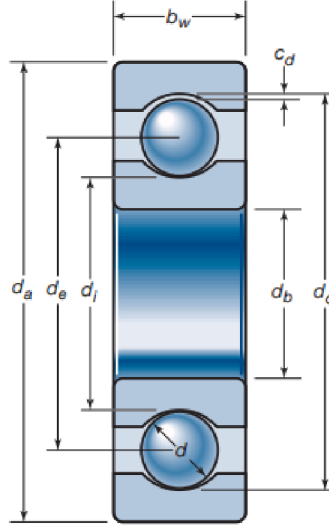


Figure 5.1: Cross section of single row ball bearing [12]

For the rolling element contact analysis are important following dimensions: outer raceway diameter  $d_o$ , inner raceway diameter  $d_i$  and ball diameter  $d$ . These parameters can be found and measured from bearing CAD models available in the online catalogues. The practical way of this process will be presented further in the text. Another necessary parameter can be determined by the following relations:

Pitch diameter  $d_e$ :

$$d_e = \frac{d_o + d_i}{2} \quad (5.3)$$

Diametral clearance  $c_d$  (marked in the figure 4.2) is thought as the maximum distance that one raceway can move in diametral direction with respects to the other, when small load is applied [12]:

$$c_d = d_o - d_i - 2d \quad (5.4)$$

Race conformity  $R_r$  is a measure of the geometrical conformity of the race and the ball in plane passing through the bearing axis [12]. It is defined as the ratio of the raceway radius and rolling element diameter. For the ideal case, the raceway radius is equal to the ball radius, thus  $R_r$  would be  $1/2$ . However the closer the race conforms to the ball, the greater is the frictional heat within the contact. The modern bearings usually have  $0.51 < R_r < 0.54$ . The race conformity ratio for the outer raceway is said to be slightly larger compared to inner raceway, with the aim to compensate the contact stresses at inner and outer raceway [12]. In the computations of thesis, the following values are considered, adopted from [15]:

- $R_{ro} = \frac{r_o}{d} = 0.53$  for outer-ring raceway
- $R_{ri} = \frac{r_i}{d} = 0.52$  for inner-ring raceway

Radius curvature for *ball-inner-race contact*:

$$\begin{aligned} R_{xi} &= \frac{d(d_e - d\cos\beta)}{2d_e} \\ R_{yi} &= \frac{R_{ri}d}{2R_{ri} - 1} \end{aligned} \quad (5.5)$$

Radius curvature for *ball-outer-race contact*:

$$\begin{aligned} R_{xo} &= \frac{d(d_e + d\cos\beta)}{2d_e} \\ R_{yo} &= \frac{R_{ro}d}{2R_{ro} - 1} \end{aligned} \quad (5.6)$$

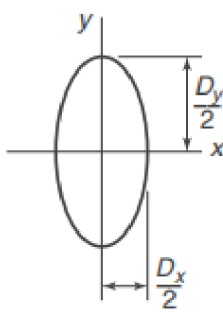
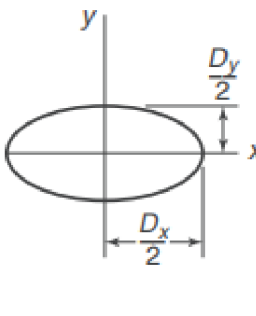
From radius curvature values of *radius ratio*  $\alpha_r$  can be obtained, for *inner-ring raceway*:

$$\alpha_{ri} = \frac{R_{yi}}{R_{xi}} \quad (5.7)$$

In analogous way for *outer-ring raceway*:

$$\alpha_{ro} = \frac{R_{yo}}{R_{xo}} \quad (5.8)$$

Value of the radius ratio determines calculation of the elliptic integrals  $\mathcal{F}$  and  $\mathcal{E}$  according to the following table 5.1:

	Radius ratio range	
Property	$1 \leq \alpha_r \leq 100$	$0.01 \leq \alpha_r \leq 1$
Geometry		
Ellipticity ratio	$k_e = \alpha_r^{2/\pi}$	$k_e = \alpha_r^{2/\pi}$
Elliptic integrals	$\mathcal{F} = \frac{\pi}{2} + \left(\frac{\pi}{2} - 1\right) \ln\alpha_r$ $\mathcal{E} = 1 + \frac{\pi-2}{2\alpha_r}$	$\mathcal{F} = \frac{\pi}{2} - \left(\frac{\pi}{2} - 1\right) \ln\alpha_r$ $\mathcal{E} = 1 + \left(\frac{\pi}{2} - 1\right) \alpha_r$

Of course, the variables ellipticity parameter  $k_e$  and consequently elliptic integrals  $\mathcal{F}$ ,  $\mathcal{E}$ , stated in the table above, are needed to be distinguished for inner and outer raceway. Final formula for curvature sum  $R$  is for *inner-ring raceway*:

$$\frac{1}{R_i} = \frac{1}{R_{xi}} + \frac{1}{R_{yi}} \quad (5.9)$$

In the same way for *outer-ring raceway*:

$$\frac{1}{R_o} = \frac{1}{R_{x_o}} + \frac{1}{R_{y_o}} \quad (5.10)$$

The estimated ellipticity parameter  $k_e$ , curvature sum  $R$  and elliptic integrals  $\mathcal{E}, \mathcal{F}$  can be finally used to calculate the elliptical contact stiffness.

### 5.1.2. Rectangular contact

Formulas for roller bearing contact stiffness is:

$$K_1 = \frac{\frac{\pi}{2} E' l}{2 \ln \left( \frac{4 R_x}{b^*} \right) - 1} \quad (5.11)$$

Used notation means:

- $E'$  effective module of elasticity
- $l$  length of the rolling element
- $R_x$  radius curvature
- $b^*$  contact semiwidth

Radius curvature for cylinder rolling elements can be calculated by formula:

$$\frac{1}{R_x} = \frac{1}{r_{a,x}} + \frac{1}{r_{b,x}} \quad (5.12)$$

Where  $r_{ax}$  denotes radius of rolling element and  $r_{bx}$  denotes radius of the bearing raceway, that value is distinguished for inner and outer raceway, consequently radius curvature  $R_x$  is distinguished in the same way, as it shows the figure below.

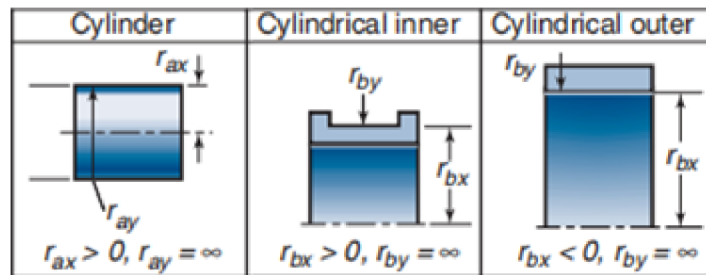


Figure 5.2: Designations for radii of curvature for rolling bearing races [12]

Contact semiwidth is given by formula:

$$b^* = R_x \left( \frac{8W'}{\pi} \right)^{1/2} \quad (5.13)$$

Here,  $W'$  is dimensionless load defined via normal load per unit  $w'$ :

$$W' = \frac{w'}{E' R_x} \quad (5.14)$$

Formula (5.14) above implies that for bearings with rectangular contact type, the radial load is necessary to be known as an input. This fact makes the stiffness estimation for the rectangular contact bearing more complicated, compared to the ball contact bearings.

### 5.1.3. Material properties

Last variable needed for contact stiffness estimation, for both cases of contact types, is effective elastic modulus, which is defined by material properties of conjugated rings and rolling elements.

$$E' = \frac{2}{\frac{1-\mu_a^2}{E_a} + \frac{1-\mu_b^2}{E_b}} \quad (5.15)$$

Where  $E$  and  $\mu$  means Young's modulus and Poisson's ratio, subscripts  $a, b$  are assigned to rolling element and bear ring, respectively.

### 5.1.4. Stiffness estimation

The stiffness of rolling bearing can be determined from contact analysis explained above together with following assumptions of loading distribution in bearing. Mostly, bearing applications involve steady-state rotation of either the inner or outer race. Furthermore, rotational speeds are usually not so high so effect as centrifugal forces or gyroscopic moments can be neglected [12].

At first, it requires to get rolling element stiffness  $K_j$ . Furthermore, the total radial deflection  $\delta_m$  is given by deflection of inner and outer ring [12]:

$$\delta_m = \delta_{mo} + \delta_{mi} \quad (5.16)$$

Here, for  $\delta_{mo}$ , and  $\delta_{mi}$  it holds:

$$\delta_{mo} = \left( \frac{w_z}{(K_j)_o} \right)^{1/j} \quad \delta_{mi} = \left( \frac{w_z}{(K_j)_i} \right)^{1/j} \quad (5.17)$$

Finally, by substituting of the equations (5.16) and (5.17) into equation (5.1) it is obtained stiffness of bearing rolling element conjunction with the inner and outer rings expressed by formula [12].

$$K_j = \frac{1}{\{[(K_j)_o]^{1/j} + [(K_j)_i]^{1/j}\}^j} \quad (5.18)$$

The value of  $j$  distinguish, if the stiffness is related to the elliptical, or rectangular conjunction shape.

## 5.2. Preloaded bearing

As have been mentioned in the review about bearing types (chapter Rolling-Element Bearings), the angular contact ball bearings are usually mounted in pairs to be able carry the thrust load. Here, it will be given a simple approach to determine the radial stiffness of the preloaded angular contact bearing. The two angular bearings are usually preloaded by mounting with rigid preload  $P$ . The figure 5.3 shows the paired bearing subjected to axial load  $A$  [16].

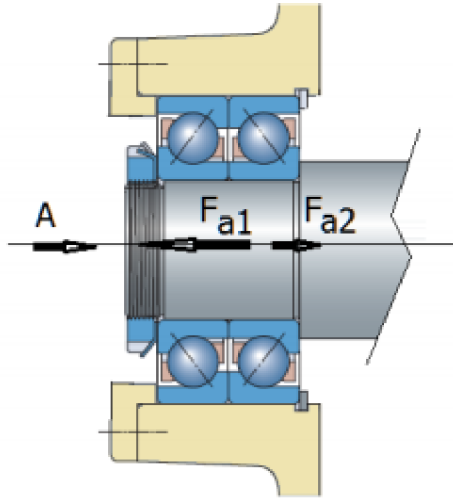


Figure 5.3: Preloaded paired bearing [16]

The mechanical equilibrium for the depicted axial bearing forces  $F_{a1}$  and  $F_{a2}$  is:

$$A = F_{a1} - F_{a2} \quad (5.19)$$

The preloaded state is special case described by equilibrium:

$$F_{a1} = F_{a2} = P \quad (5.20)$$

The initial axial deflections  $\delta_{a1}$  and  $\delta_{a2}$  of the paired bearings satisfy the relation for relative approach of the rings under the preload [16]:

$$\delta_{a1} + \delta_{a2} = e \quad (5.21)$$

The equations stated above can be illustrated by preload deflection curve stated in the figure 5.4. The graph shows that value of  $P$  corresponds with the intersection of two opposite curves when equation (5.20) holds.

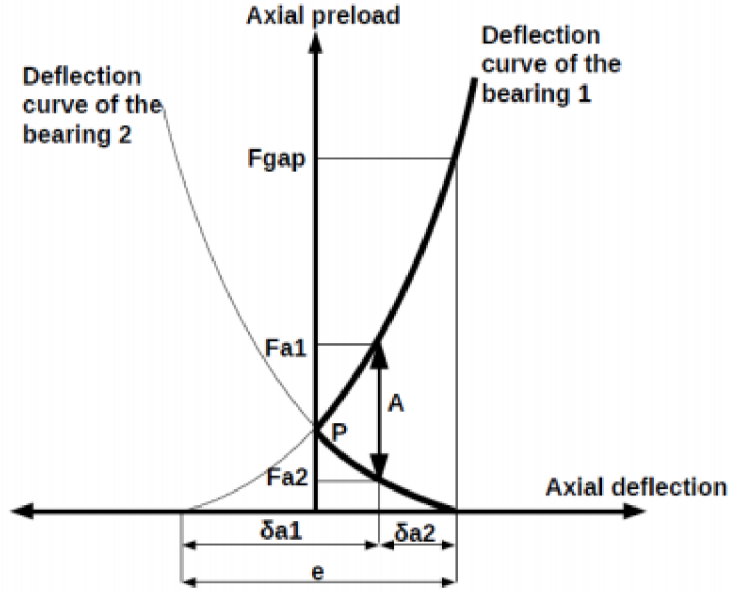


Figure 5.4: Deflection curve for paired bearing [16]

In accordance with the analysis stated in [16], relation for preload  $P$  holds:

$$P = Z \cdot K_j \cdot \sin^{5/2}(\beta) \cdot (e/2)^{3/2} \quad (5.22)$$

Finally, it can be estimated, according to the paper in [16], that the axial stiffness  $k_a$  and the radial stiffness  $k_r$  of the paired bearing is:

$$k_a = 3 \cdot (Z \cdot K_j)^{2/3} \sin^{5/3}(\beta) \cdot P^{1/3} \quad (5.23)$$

$$k_r = \frac{k_a}{\tan^2(\beta)} \quad (5.24)$$

The aim of the calculations stated in this chapter is to show how the bearing stiffness can be determined for the machine designer as simply as possible. The only parameters needed for the input are outer raceway diameter  $d_o$ , inner raceway diameter  $d_i$ , ball diameter  $d$ , and the number of rolling elements  $Z$  which are accessible from bearing catalogues, and the CAD geometry. There have been developed several other approaches to estimate the bearing stiffness, which are usually based on experimental analysis. Their potential use with the results comparison will be discussed in later chapter Application, dedicated to practical rotor analysis.

# 6. Power losses

This chapter covers phenomenon of friction heat generated in shaft bearings. There exist various sources of frictional resistance. The most predominating cases will be discussed, with the mathematical approach to describe them.

Quantitative evaluation of the total power dissipated in bearing can be expressed by formula [13]:

$$P_{dis} = M \cdot \frac{2\pi}{n} \quad (6.1)$$

Where,  $n$  denotes operational speed of the bearing in revolution per minute,  $M$  gathers total frictional momentum arising from bearing component contacts and lubricant interaction. In detail the frictional momentum can be expanded as follows [13]:

$$M = M_P + M_L + M_S \quad (6.2)$$

The terms in equation above express the load dependent momentum  $M_P$ , lubricant viscous friction momentum  $M_L$ , and sealing friction momentum  $M_S$  [13].

## 6.1. Loading friction

Loading contact friction consists of two major contributing factors: rolling and sliding. First one, rolling, is caused by elastic hysteresis. When roller and raceway materials just ahead of the contact in the circumferential direction undergo distortion and compression, while, material just behind the contact is relieved of stress. Second factor, sliding, is a microslip which occurs in the rolling direction as a result of roller depression and raceway stretch. The deformation causes the roller goes forward slightly less than its circumference in one revolution [13].

The total frictional momentum can be evaluated within sufficient accuracy as a load and geometry dependent using a constant coefficient of friction [13]:

$$M_P = 0.5 \cdot \mu \cdot d_b \cdot P \quad (6.3)$$

Used notation means:

- $M_P$  bearing frictional momentum
- $\mu$  coefficient of the friction for the bearing
- $P$  equivalent static load
- $d_b$  bearing bore diameter

The equivalent static load  $P$  can be estimated based on axial  $F_a$  and radial  $F_r$  bearing reactions in accordance with the procedure stated in [17] with the following relations:

$$\begin{aligned} \frac{P}{F_r} &= 1 \quad \text{for } \frac{F_a}{F_r} \leq e \\ \frac{P}{F_r} &= X + Y \frac{F_a}{F_r} \quad \text{for } \frac{F_a}{F_r} \geq e \end{aligned} \quad (6.4)$$

As radial load  $F_r$  is considered obtained bearing reaction from static analysis computation, axial load  $F_a$  can be obtained from additional computations, not directly from bended beam static analysis. Coefficients  $X$  and  $Y$  denote radial load and axial load factors. The values of these coefficients together with the value for limit value  $e$  can be found in bearing catalogue. Another required input is static load rate  $C_0$  and mutual position of the shaft bearings. Possible cases of the bearings' position are: single or paired in tandem, especially for angular contact ball bearings plays role, if they are set up to each other in opposite position in "X", or "O" [17].

This case of friction predominates in cases with slow rotation and heavy loads [13].

## 6.2. Lubricant friction

Lubricant friction arises from interaction of roller and viscous shearing on rolling element, cage and raceway surfaces and churning on lubricant dispersed in bearing cavity [13].

The lubricant friction momentum can be expressed as follows [13]:

$$\begin{aligned} M_L &= 10^{-7} \cdot f_L \cdot (\nu \cdot n)^{2/3} \cdot d_m^3 & \text{for } \nu \cdot n > 2000 \\ M_L &= 160 \cdot 10^{-7} \cdot f_L \cdot d_m^3 & \text{for } \nu \cdot n < 2000 \end{aligned} \quad (6.5)$$

Used notation means:

- $M_L$  momentum representing lubricant losses
- $\nu$  lubricant kinematic viscosity
- $n$  bearing speed
- $f_L$  factor depending on bearing type and method of lubrication

This case of friction is typical for applications with high speeds and light loads.

## 6.3. Sealing friction

Sliding motion in contact of the cage and rollers, or sliding between the end of rollers and seal can appear in bearing. In such cases for the sealing friction momentum the empirical equation holds [13]:

$$M_S = \left( \frac{d_b + D}{f_1} \right)^2 + f_2 \quad (6.6)$$

Used notation means:

- $M_S$  friction momentum of two seals
- $d_b, D$  bearing bore diameter, outside diameter
- $f_1, f_2$  friction factors for bearing seals, dependent on bearing design

This case of friction loss is worth to be considered when inadequate lubricant is used the kinematic viscosity is high, or the operating temperatures are low [13].

Values of the bearing coefficients, in the formulas above, are stated in the appendix Frictional coefficients.

# 7. Software interface

As the objectives of this thesis set, one of the points of the assignment is to develop a simple software to analyze the rotor system. The devised software is required to include the whole theory summarised in the previous chapters. This chapter will give a review into software developing tools that can be considered to built up a graphical user interface (GUI).

## 7.1. MATLAB

MATLAB is a popular tool for scripting and computations in scientific and engineering applications. The language is math oriented, which makes it useful for engineering computations based especially on matrix calculus. Another worthy advantage of MATLAB is, that it provided several specialized toolboxes (GUI based applications) , which make the scientific computing for the users even more convenient. The toolboxes and the scripting language are professionally developed, rigorously tested and documented for scientific usage, which are the reasons, it has to be paid for a use of this software.

Since 2015, MATLAB has released a new environment called App Designer, through which the user can develop a specific interface based on his own preferences and purposes. The advantages of the MATLAB GUI build up environment are following: relatively easy to learn, develop and set up the apps even for users less experienced with GUI designing.

## 7.2. Python

Python can be an open source alternative to MATLAB. However, since Python is more general purpose programming language, it demands intermediate programming skills of the user. Compared to the MATLAB toolboxes testing, user can rely on community developed function packages and libraries available on web forums. On the other hand, since the Python is open source, there is no official guaranty of the language usage for certain purposes like it is for MATLAB. In terms of application development, there exists PyQt5 Designer, which is solid environment to build up a custom app, similar to MATLAB App Designer. However, it is suitable rather for basic apps, than more visual wise complex applications.

## 7.3. C++

C++ is general purpose, object oriented programming language that scales up huge range of applications like software, websites, or algorithm developing. The syntax is much more complex, compared to MATLAB or Python, which requires higher level of software knowledge and programming skills of the user. If the goal is to develop tools for certain data analysis or model building, of course it can be done in C++, but process can be much more harder and time consuming for users less experienced with software development.

# 8. Rotor shaft solver

Based on the review above, it was decided to use MATLAB App Designer environment to build up a software solver for rotor analysis. The figure 8.1 shows the layout structure of the developed application divided into two major parts. Upper part contains a tab group panel with three tabs: Input, Shaft Results, and Bearing Results. In the lower part, there are situated two panels called Shaft and Control, to visualize the solved rotor and control the opened project.

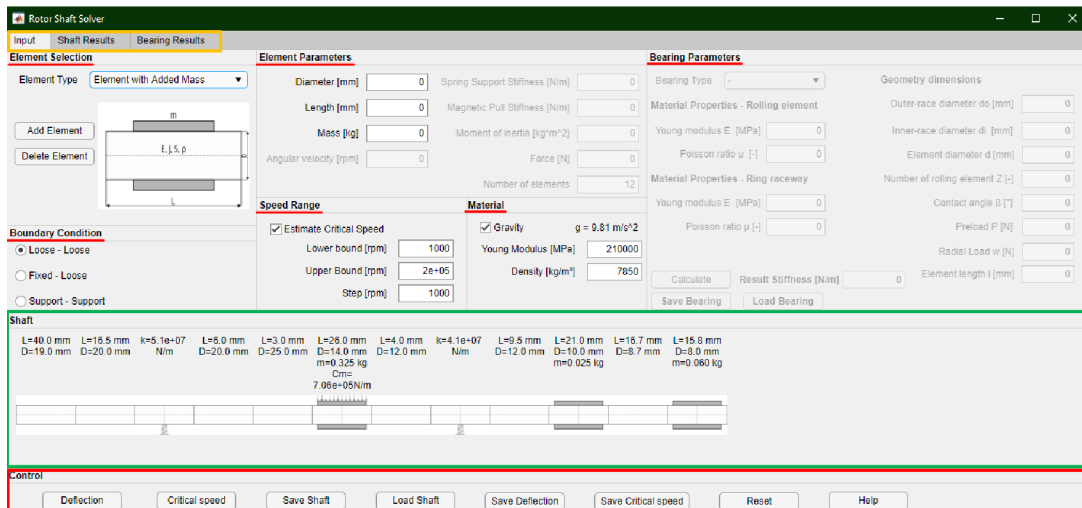


Figure 8.1: Solver layout, with filled example

The following section explains shortly the idea of the user work-flow of the developed program. Three basic parts of the work-flow can be considered, rotor parameters definition and possible outcomes, detailed bearing results analysis, and project data save.

The following picture illustrates the basic idea of the program work-flow.

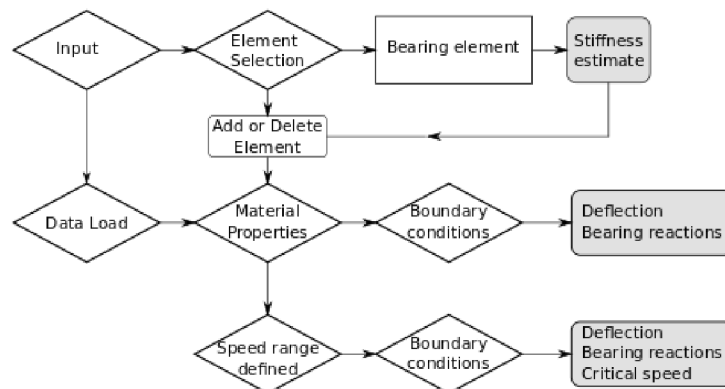


Figure 8.2: Scheme of the rotor definition and obtained results

According to the scheme 8.2, an input of the rotor parameters is required at the beginning. There are two options, first is to define the array of specific element types, second is to load rotor defining parameters saved from the previous use of the program. With the buttons *Add Element* or *Delete Element* is possible to edit the sequence of the rotor elements. Of course the, element array loaded from a saved file can be edited. Bearing element has

specific input parameters requirements to estimate the bearing contact stiffness located in the panel *Bearing Parameters*. User can save, or load the bearing parameters via the separate file, dedicated to specify bearing input parameters.

After the elements array is defined, the material properties of the rotor have to be defined: material density, and Young modulus. Material density input plays an important role in the calculation, it determines what can be gained as an outcome of the analysis.

If the material density is not specified in accordance with the transfer matrix formulas (appendix Transfer matrices), the shaft mass load distribution is neglected and only the deflection shape function and bearing reactions can be obtained. Only if the density has been specified, the critical speed analysis is possible as an outcome.

To take into account the phenomenon of the mass load distribution except for material density also gravity influence has to be considered in the calculation. As the scheme 8.2 shows, if the density is not included in the analysis, the resulting deflection shape function does not reflect the shaft mass distribution, however the influence of the gravitational force of the beared masses can be included in the calculation. If both, the material density and gravity acceleration, are included in the analysis inputs, the resulting deflection shape function reflects the shaft mass distribution along the rotor axes.

For the critical speed estimation the gravity influence is not relevant input parameter.

To decide if the mass load distribution should be considered in the computation, it determines how the rotor is oriented in reality. If the rotor is mounted horizontally, it is appropriate to consider the mass distribution influence. If the rotor is vertically oriented, the mass distribution is not relevant for the analysis of the transverse bended beam body.

The chain in the scheme 8.3 illustrates the procedure of the bearing power loss analysis. Since the bearing reaction forces have been estimated, the results can be used to compute the induced heat in the chosen bearing according to the theory stated in the chapter Power losses. User can decide if the cases *lubricant*, or *sealing* friction should be taken into account in the heat loss analysis.

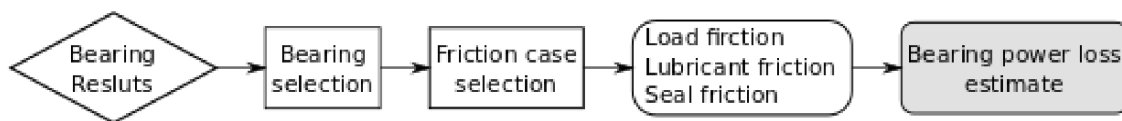


Figure 8.3: Scheme of the bearing results analysis

The last chain, figure 8.4, illustrates that in the current project opened in the program there can be saved several specific files, which can be useful for further analysis, or obtained result processing, or analysis repetition. The input parameters for the computation can be saved into file with MATLAB suffix *.mat*. There are three options. User can decide to save the rotor definition into file named *Shaft\_Data.mat*, another option is to save inputs to store bearing contact stiffness inputs into the file *Bear\_Param.mat*, or to save the parameters for the heat analysis for the selected bearing into the file *Heat\_Param.mat*. For the results, there is an option to store computed deflection, and critical speed curves

into *.txt* files. The bearing results gathered in the final table, situated in the panel *Bearing Results*, can be exported into Excel *.xlsx* file.

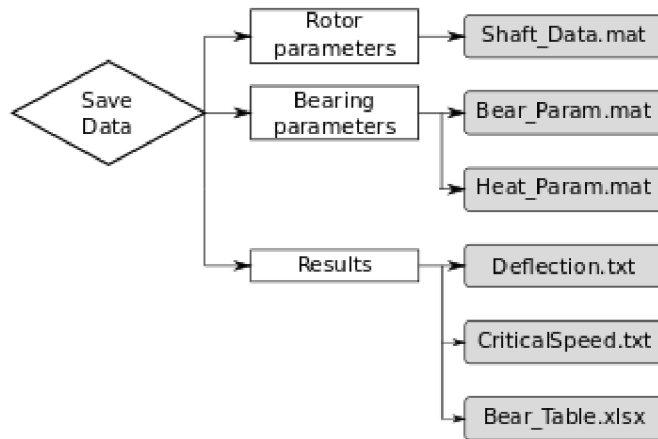


Figure 8.4: Scheme of the data save

The description above gives only a brief insight into the program work-flow, the following sections explain the structure of the program components in more detail. The components can be distributed into the following categories, based on the purpose to be used for. The categories are: input parameters components, results and visualizing components, and project control buttons.

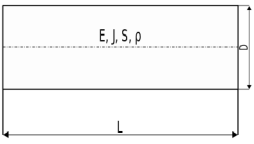
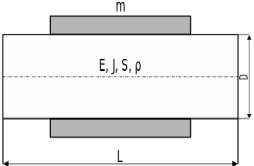
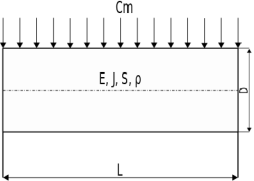
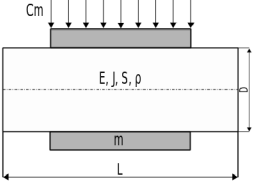
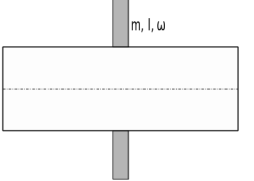
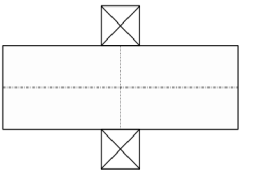
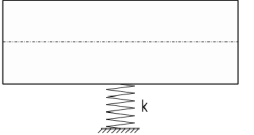
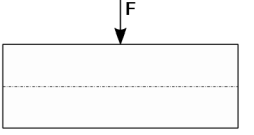
## 8.1. Input parameters

The tab group *Input* serves to define the initial properties of the solved rotor. The following panels have to be used: *Element Selection*, *Element Parameters*, *Bearing Parameters*, *Boundary Conditions*, *Speed Range*, and *Material*.

### 8.1.1. Elements definition

In the panel *Element selection*, there is a drop down menu, containing a list of possible rotor element types. The following table 8.1 contains the element types with the relevant input parameters. The list is in accordance with elements list stated in the appendix Transfer matrices. Buttons *Add Element* and *Delete Element* serve to control the elements sequence definition. Already defined elements are shown in the panel *Shaft*.

Table 8.1: List of the element types with required parameters

Element type	Picture	Parameters	Unit
Shaft element		Diameter Length	[mm] [mm]
Element with added mass		Diameter Length Mass	[mm] [mm] [kg]
Magnetic pull		Diameter Length Magnetic pull stiffness	[mm] [mm] [N/m]
Magnetic pull and added mass		Diameter Length Mass Magnetic pull stiffness	[mm] [mm] [kg] [N/m]
Disc		Mass Moment of inertia Angular velocity	[kg] [kg · m <sup>2</sup> ] [rpm]
Bearing		Stiffness estimated in panel Bearing parameters	[N/m]
Spring Support		Spring stiffness	[N/m]
Force		Transverse force	[N]

## 8.1.2. Bearing parameters

This panel, shown in the figure 8.5, serves to estimate the bearing element contact stiffness in accordance with the process stated in chapter Bearing stiffness. The elements become active when the option *Bearing* from the element drop down menu *Element Type* is chosen.

Figure 8.5: Panel with for bearing stiffness estimation

After that can be chosen the *Bearing Type*, *Ball Bearing*, *Roller Bearing* or *Preloaded Paired Bearing*. In accordance with the selected bearing type corresponding input fields become active to use, as shows the following table.

Table 8.2: Bearing type input parameters

Inputs requested for	Parameter	Mark	Unit
Ball bearing and roller bearing	Outer-race diameter	$d_o$	[mm]
	Inner-race diameter	$d_i$	[mm]
	Element diameter	$d$	[mm]
	Contact angle	$\beta$	[°]
Roller bearing	Radial load	$w$	[N]
	Element length	$l$	[mm]
Preloaded pair bearing	Number of rolling elements	$Z$	[-]
	Preload	$P$	[N]

When the proper parameters for the chosen bearing type are filled in, the *Result Stiffness* of the bearing can be calculated. After that the bearing element with estimated stiffness can be added into the rotor elements array using the button *Add Element* as done for the others element types.

### 8.1.3. Material and Speed Range

In the panel *Material* Young modulus and shaft material density is defined. Moreover, user can decide via the check box *Gravity*, if the effect of the mass distributed along the shaft axis and causing gravity forces should be considered in the computation, as has been explained in the previous section.

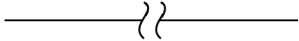
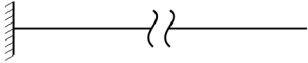
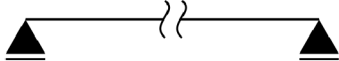
Under the panel *Speed Range* user can define the range of the operational speed to estimate the critical speed of the rotor, according to the process explained in the chapter Beam computations, section Dynamic response. Requested inputs for the interval are: *Lower bound*, *Upper bound* and *Step*.

Speed Range		Material	
<input checked="" type="checkbox"/> Estimate Critical Speed		<input checked="" type="checkbox"/> Gravity	g = 9.81 m/s <sup>2</sup>
Lower bound [rpm]	<input type="text" value="1000"/>	Young Modulus [MPa]	<input type="text" value="210000"/>
Upper Bound [rpm]	<input type="text" value="1.5e+05"/>	Density [kg/m <sup>3</sup> ]	<input type="text" value="7850"/>
Step [rpm]	<input type="text" value="1000"/>		

Figure 8.6: Detail of the panel *Speed Range* and *Material*

### 8.1.4. Boundary conditions

The panel named *Boundary Conditions* contains buttons for choosing appropriate boundary conditions for the transfer matrix algorithm. The most common cases of the mounting state of the rotor considered are grouped in the following table.

Table 8.3: Possible boundary conditions	
Condition	Scheme
Loose - Loose	
Fixed - Loose	
Support - Support	

## 8.2. Shaft visualize

The panel *Shaft* serves to visualize simply the scheme of the rotor according to the elements' selection. Above the elements' schematic pictures, there are stated labels with element specific parameters.

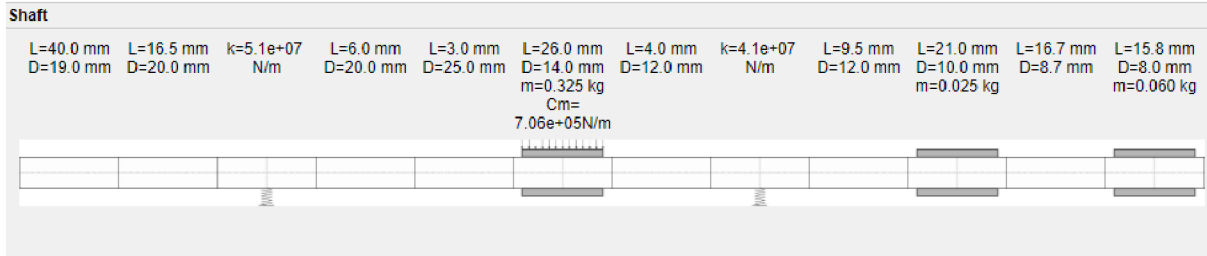


Figure 8.7: Visualized shaft scheme

## 8.3. Shaft Results

This tab panel contains a graph to plot deflection curve, and numeric field containing the maximal deflection, which is also highlighted in the deflection graph. That outcome can be obtained as a callback of the push button *Deflection*.

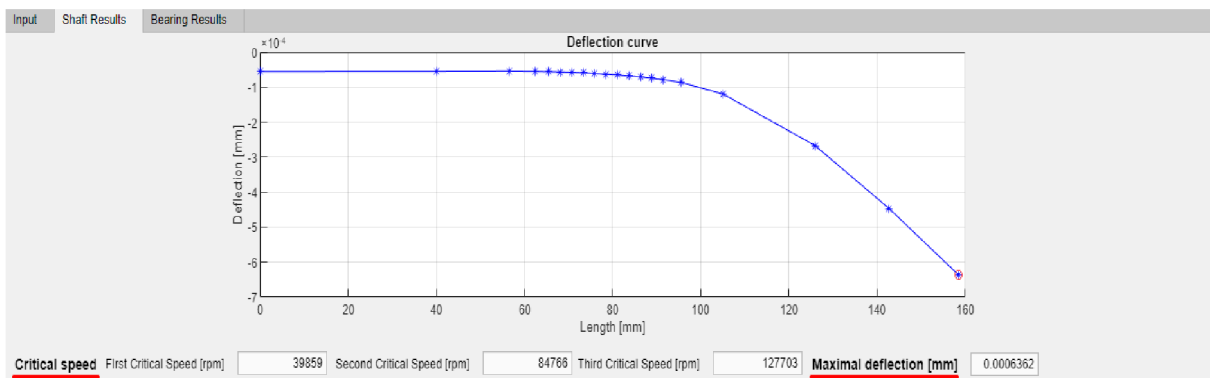


Figure 8.8: Shaft result panel

As a callback to the *Critical Speed* push button can be obtained at most first three values of the critical speed, printed in three numeric fields under the graph. In the graph user can observe the determinant in dependency on the given speed range to look if more than three critical speeds in the range can occur.

## 8.4. Bearing Results

In the tab panel *Bearing Results* is situated a table containing following columns *Select*, *Reaction*, *Deflection*, *Stiffness*, and *Power loss*. The order of the bearing numbering is meant from left end of the shaft up to the right end. The force reactions are obtained from the deflection computation.

Input	Shaft Results	Bearing Results						
<b>Force Reaction</b>								
Select	Reaction [N]	Deflection [mm]	Stiffness [N/m]	Power loss [W]				
1 <input checked="" type="checkbox"/>	2.7496	5.3913e-05	51000000	5.4645				
2 <input type="checkbox"/>	3.5389	8.6315e-05	41000000	0				
<b>Power loss</b>								
Radial Load [N]	<input type="text" value="2.75"/>	Static load rating [N]	<input type="text" value="9500"/>	<input checked="" type="checkbox"/> Lubrication <input type="checkbox"/> Sealing				
Axial Load [N]	<input type="text" value="0"/>	Radial load factor X	<input type="text" value="0.26"/>	Kinematic viscosity [mm <sup>2</sup> /s]	<input type="text" value="96"/>	Factor f1 [-]	<input type="text" value="0"/>	
Bore diameter [mm]	<input type="text" value="20"/>	Axial load factor Y	<input type="text" value="0"/>	Lubrication factor fl [-]	<input type="text" value="2"/>	Factor f2 [-]	<input type="text" value="0"/>	
Constant factor μ	<input type="text" value="0.0015"/>	Limiting value e	<input type="text" value="1.14"/>	Pitch diameter dm [mm]	<input type="text" value="36"/>	Outer Diameter D [mm]	<input type="text" value="0"/>	
Revolution n [rpm]	<input type="text" value="1800"/>	Position	<input type="text" value="In Tandem"/>					
<input type="button" value="Calculate"/>		Heat Loss [W]	<input type="text" value="5.465"/>	<input type="button" value="Save Heat"/>		<input type="button" value="Load Heat"/>		<input type="button" value="Save Table"/>

Figure 8.9: The panel gathering the bearing results

The power loss generated in the certain bearing can be estimated in panel *Power loss* situated below the table. The chosen bearing can be picked up in the table, and as the radial load will be taken resulting radial bearing reaction, stated in the table. After that, following inputs for the resulting frictional momentum are necessary to be filled in:

Table 8.4: Load friction inputs

Parameter	Mark	Unit
Radial load	$F_r$	[N]
Axial load	$F_a$	[N]
Bore diameter	$d_b$	[mm]
Friction constant	$\mu$	[-]
Operating revolution	$n$	[rpm]
Static load rating	$C$	[N]
Radial load factor	$X$	[-]
Axial load factor	$Y$	[-]
Limiting value	$e$	[-]
Position		[-]

If the influence of the bearing lubricant is to be considered in the analysis, there is a checkbox called *Lubrication*. If the checkbox is checked off, the following inputs fields will be activated:

Table 8.5: Lubrication friction inputs

Parameter	Mark	Unit
Kinematic viscosity	$\nu$	[mm <sup>2</sup> /s]
Lubrication factor	$f_l$	[-]
Pitch diameter	$d_e$	[mm]

If the influence of the bearing sealing is to be considered in the analysis, there is another checkbox called *Sealing*. If the checkbox is checked off, the following inputs fields will be activated:

Table 8.6: Sealing friction inputs

Parameter	Mark	Unit
First sealing factor	$f_1$	[-]
Second sealing factor	$f_2$	[-]
Outer diameter	$D$	[mm]

The parameters can be saved into *Heat\_Param.mat*, if they have been filled in, via the button *Save Heat*. Of course, they can be also uploaded from the previous computations via the button *Load Heat*.

As the heat loss has been computed, as a callback to the *Calculate* push button, the value is assigned to the last column in the row for the selected bearing. Furthermore, the table gathering the bearing results can be exported to *.xlsx* file via push button *Save Table*, as the figure 8.9 depicts.

## 8.5. Project control

The last panel named *Control* includes push buttons that allows the calculations and project data control. There are also some other push buttons in the program to control some computations or data parameters control. That all will be described in the following paragraphs.

### 8.5.1. Computation

The two buttons *Deflection* and *Critical speed* serves to obtain a deflection curve with the bearing force reactions, and critical speeds, respectively. The response will appear in the tab *Shaft Results* (defection curve and critical speed curve and values) and in the panel *Bearing Results* (the bearing reaction forces). As has been explained in the previous sections.

To obtain the correct deflection results the following parameters have to be filled in properly:

- Element selection and relevant parameters definition, especially for the bearing stiffness estimation
- Boundary conditions with correctly chosen option
- Material properties, where Young modulus is always necessary, density with gravity are optional (as explained in the introduction of this chapter)

To obtain the correct critical speed results the following parameters have to be filled in properly:

- Element selection and relevant parameters definition, especially for the bearing stiffness estimation
- Boundary conditions with correctly chosen option

- Material properties, where Young modulus is always necessary, density for critical speed analysis is also necessary, gravity influence is not relevant
- Speed range, where range bounds with the interval step need to be filled in

Another calculation push button is situated in the panel *Bearing parameters*, when the bearing contact stiffness is obtained as a callback. To get the *Result Stiffness* all active numeric fields need to be filled in, for chosen bearing type.

There is also calculation push button situated in the tab *Bearing results*, panel *Power loss*, which serves to estimate the power loss for bearing selected in the table .

### 8.5.2. Data save

It is possible for the user to save the current project via push button *Save Shaft*. As a response, the dialogue box will appear to save the project data file. By default the file name is set as *Shaft\_Data.mat*. The structure of the created file is illustrated in the following figure.

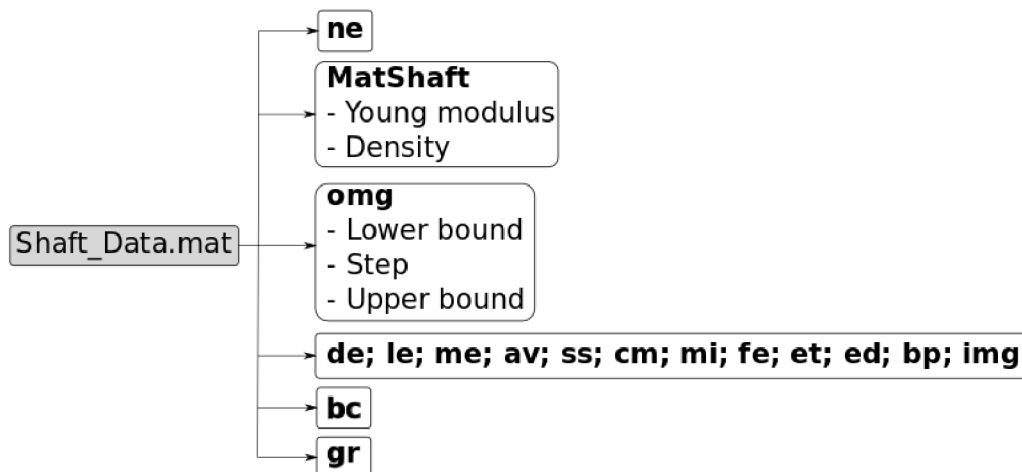


Figure 8.10: Data structure of the rotor definition saved file

The notation used in the figure above has the following meaning: parameter **ne** means number of the rotor elements in the project, parameter **MatShaft** includes values of Young modulus and material density. Parameter **omg** is used to save data about speed range definition, if the check box *Estimate critical speed* is filled, the first value of the variable **omg** is 1, the others are parameters of the speed range. If the check box is not filled, the first value is 0 and the other values are 0 as well. The fourth array of

variables in the figure 8.10 contains data about elements' parameters, the meaning is:

- **de** element diameter
- **le** element length
- **me** element added mass
- **av** angular velocity
- **ss** saved spring support, or bearing stiffness
- **cm** magnetic pull stiffness
- **mi** moment of inertia
- **fe** value of the transverse force
- **et** element type
- **ed** label of element description
- **bp** bearing, or spring support position index
- **img** element schematic picture

The remaining parameters **bc** and **gr** include the information about selected boundary conditions, and gravity check box.

Naturally, if the user had saved the project data sometimes before, there is an option to load the saved data file to continue or correct some previous analysis. This can be done via push button *Load Shaft*. As a response the saved rotor will appear visualized in the *Shaft* panel with corresponding labels. Also boundary conditions, material properties specifications eventually speed range definition values will correctly fill in.

Another save and load push buttons control are available in the panel *Bearing parameters*. The user can save entered bearing parameters, with corresponding selected bearing type, for eventual upcoming calculations. The file name for bearing save is by default set as *Bear\_Param.mat*. The structure is show in the figure below.

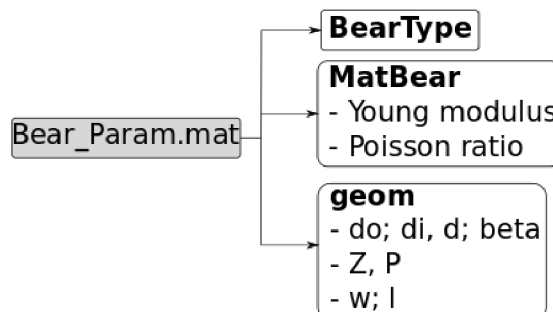


Figure 8.11: Data structure of the bearing definition saved file

The meaning of the structure, in the figure 8.11, is following. Variable **BearType** contains the label of the selected bearing type from the drop down menu: *Ball Bearing*, *Roller*

*Bearing*, and *Paired Preloaded*. Variable **MatBear** includes material properties of the rolling elements and bearing ring raceways. The first and second values relate to Young modulus of the rolling elements, and the rings, respectively. The third and fourth values of this variable relate to the Poisson ratios of the rolling elements, and the rings, respectively. Variable **geom** consists of geometry parameters of the bearing. The content of this variable depend on the selected bearing, as it is depicted in the third block in the figure 8.11. The parameters in the first row mean:

- **do** Outer-ring raceway diameter
- **di** Inner-ring raceway diameter
- **d** Rolling element diameter
- **beta** Contact angle

The first row is common for all bearing types. If the *Paired Preloaded* bearing type is selected, the second row in saved file is included containing the parameters about number of rolling elements **Z**, and bearing preload **P**. The last row is related to the bearing type *Roller Bearing* containing the values with the following meaning bearing radial load **w**, and rolling element effective length **l**.

The last file save and load push buttons control are related to bearing power loss analysis in the panel *Bearing Analysis*, the structure of the saved file is depicted in the figure 8.12 bellow.

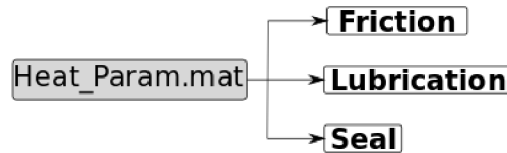


Figure 8.12: Data structure of the heat loss parameters saved file

The meaning of the variables in the saved file *Heat\_Param.mat* is as follow. The variable **Friction** contains parameters related for friction momentum calculation, the sequence of the values stored in the variable is explained below:

- $F_r$  Radial load
- $F_a$  Axial load
- $d_b$  Bearing bore diameter
- $\mu$  Friction constant factor
- $n$  Bearing operating revolution
- $C_o$  Static load rating
- $X$  Radial load factor
- $Y$  Axial load factor
- $e$  Limiting value
- *Position* Label of the bearing position for dynamic load calculation

If the the lubrication is taken into account for the analysis, the variable **Lubrication** is nonzero containing the sequence of the following values:

- $\nu$  Grease kinematic viscosity
- $f_l$  Lubrication factor
- $d_m$  Bearing pitch diameter

The last variable **Sealing** is nonzero, if the sealing impact is said to be considered in the analysis, and contains the following sequence of the variables related to sealing momentum induced in the bearing:

- $f_1$  First sealing factor
- $f_2$  Second sealing factor
- $D$  Bearing outer diameter

## 8.6. Warning dialogues

As explained in the introduction section of this chapter, in dependency of desired outcomes, appropriate inputs need to be entered. The program is designed to alert the user if some inputs are incorrectly entered. The aim is to preserve potential erroneous calculations. Here is given an overview of such situation.

**Missing Young modulus:** This parameter is always requested for both deflection and critical speed analysis. If the related numeric field is empty, the following warning will appear.

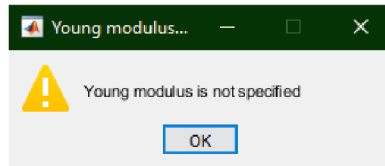


Figure 8.13: Warning dialogue about Young modulus

**Missing material density:** This parameter is important for critical speed analysis. So, if button *Critical speed* is pushed and the density numeric field is empty, the warning dialogue will appear.

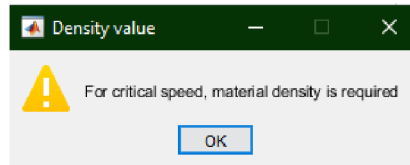


Figure 8.14: Warning dialogue about material density

**Missing Speed Range values:** If the user requests again critical speed results, but the Speed range parameters are empty, program will inform the user to specify the range.

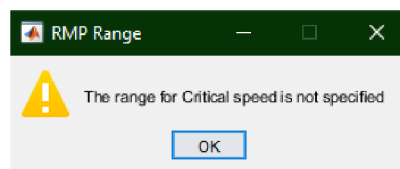


Figure 8.15: Warning dialogue about Speed range

**Incorrect boundary conditions:** Such situation can occur, if there is not specified element type called *Spring Support*, or *Bearing* and concurrently boundary conditions *Loose - Loose* is chosen. Consequently, the transfer matrix of the rotor would become singular and the algorithm would break down. To preserve such occurrence, the following dialogue warns the user to change the boundary conditions, or redefine the rotor elements.

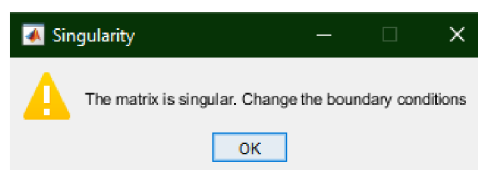


Figure 8.16: Warning dialogue about possible singular matrix

**Missing specific parameters:** Such warning will appear in the following cases:

- some parameter for chosen element has not been specified before adding selected element type
- bearing stiffness is requested, but some parameter has not been entered
- bearing power loss is requested, but some requested parameter has not been specified

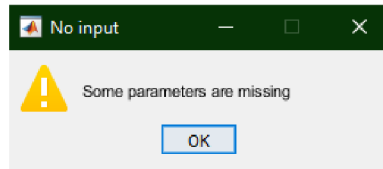


Figure 8.17: Warning dialogue about missing specific parameter

**Missing rotor definition** This warning will alert the user, if there is no rotor element defined, and concurrently one of the *Deflection*, *Critical speed*, or *Save Shaft* button is pushed.

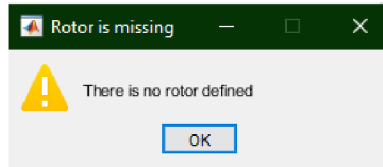


Figure 8.18: Warning dialogue about missing rotor definition

## 8.7. Software installation

The procedure to run developed program is to run *.m-file* script appended to this thesis from running MATLAB script window. The necessity is to have the script in the same folder with the added figures to visualize of the rotor element types.

For more convinced regular use of the software, the script with the pictures can be packed in to *.mlappinstall* file via button *Package App* in the MATLAB window. After that, the packed file can be via button *Install App* uploaded between other available MATLAB toolboxes.

The script of the application is designated without any dependency on another MATLAB toolboxes. No additional toolbox is required to be installed to run the application.

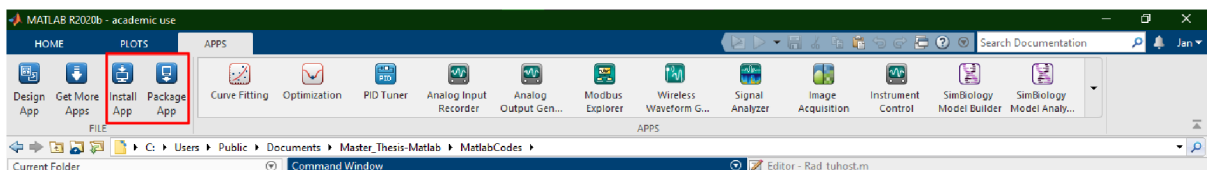


Figure 8.19: Application package and install buttons location, in MATLAB window

# 9. Application

This chapter is devoted to show a practical example of the specific rotor analysis, to illustrate the use developed software. Moreover, it will be discussed the impact of the different approaches to model the bearing stiffness to the final results.

## 9.1. Solved rotor

The scheme, figure 9.1, depicts the rotor, adopted from [4], which will be solved in this chapter.

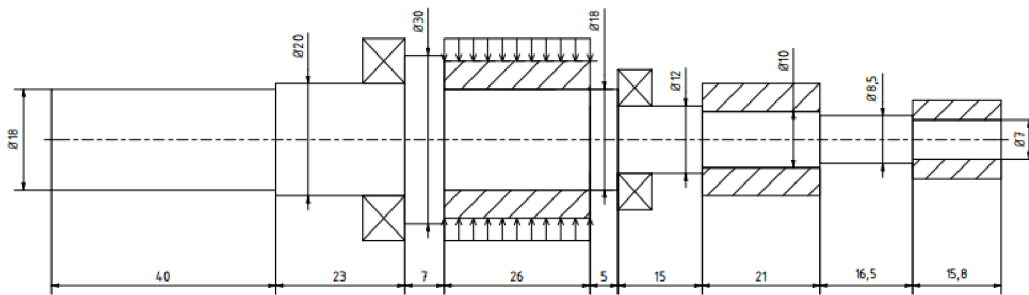


Figure 9.1: Drawing scheme of the solved rotor AF 502-B

The other figure 9.2 shows the the mentioned rotor as a sequence of the discreet elements for the transfer matrix algorithm. It can be seen, there are 13 elements, when the bearings are replaced by spring support and the shaft element type with the width corresponding to the one half of the bearing width is added between the bearing and the adjoining element (elements no. VI., and no. VIII.). The estimation of the spring (bearing) stiffness is commented on in further detail below.

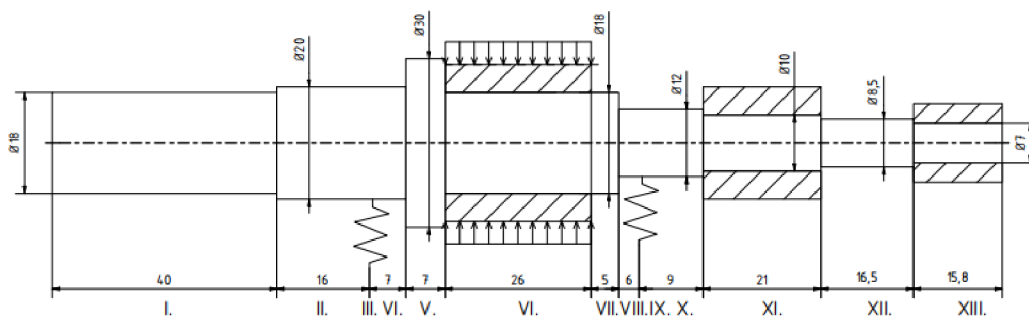


Figure 9.2: Scheme of the solved rotor AF 502-B for transfer matrix algorithm

The following table 9.1 gathers used rotor elements types with the specific parameters' values.

Table 9.1: Solved rotor parameters

Element type	Parameters	Value	Unit
Shaft element	Diameter	$D$	19 [mm]
	Length	$L$	40 [mm]
Shaft element	Diameter	$D$	20 [mm]
	Length	$L$	16 [mm]
Bearing	SKF 7304 BE-2RZP		
Shaft element	Diameter	$D$	20 [mm]
	Length	$L$	7 [mm]
Shaft element	Diameter	$D$	30 [mm]
	Length	$L$	5 [mm]
Element with magnetic pull and added mass	Diameter	$D$	18 [mm]
	Length	$L$	26 [mm]
	Mass	$m$	0,625 [kg]
	Magnetic pull	$C_m$	706000 [N/m]
Shaft element	Diameter	$D$	18 [mm]
	Length	$L$	5 [mm]
Shaft element	Diameter	$D$	12 [mm]
	Length	$L$	6 [mm]
Bearing	SKF 7301 BE-2RZP		
Shaft element	Diameter	$D$	12 [mm]
	Length	$L$	9 [mm]
Shaft element with added mass	Diameter	$D$	10 [mm]
	Length	$L$	21 [mm]
	Mass	$m$	0,025 [kg]
Shaft element	Diameter	$D$	8,5 [mm]
	Length	$L$	16,5 [mm]
Shaft element with added mass	Diameter	$D$	7 [mm]
	Length	$L$	15,8 [mm]
	Mass	$m$	0,06 [kg]

### 9.1.1. Bearing stiffness calculation

The chosen bearings for solved rotor are angular contact ball bearing SKF 7304 BE-2RZP, and SKF 7301 BE-2RZP. The figure 9.3 shows the geometry of the selected bearings, obtained from CAD model available in the online catalogue on the website of SKF. In the figure there are marked the dimensions necessary for the bearing stiffness estimation, and the induced power losses analysis, based on the formulas stated in the chapters Bearing stiffness, and Power losses, respectively.

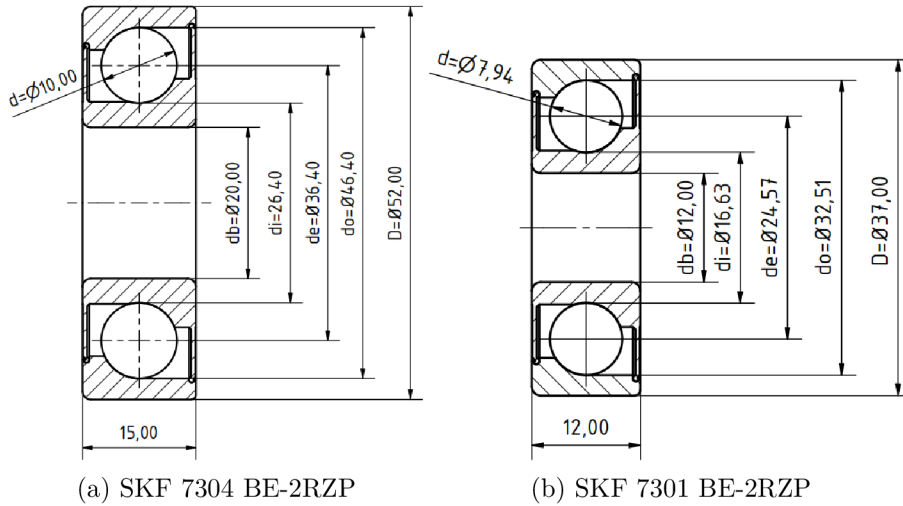


Figure 9.3: Selected bearings geometry

The parameters needed for the calculation are grouped in the table 9.2. The value of the contact angle  $\beta_f$  is chosen in accordance with the bearing data available in the online SKF catalogue.

Table 9.2: Selected bearings parameters

Parameter	SKF 7304 BE-2RZP		SKF 7301 BE-2RZP		
	Value	Unit	Value	Unit	
Outer-raceway diameter	$d_o$	46,4	[mm]	32,52	[mm]
Inner-raceway diameter	$d_i$	26,4	[mm]	16,63	[mm]
Element diameter	$d$	10	[mm]	7.94	[mm]
Pitch diameter	$d_e$	36.4	[mm]	24.57	[mm]
Outer diameter	$D$	52	[mm]	37	[mm]
Contact angle	$\beta_f$	40	[°]	40	[°]
Number of rolling elements	$Z$	9	[-]	8	[-]
Young modulus, the rings	$E$	210 000	[MPa]	210 000	[MPa]
Young modulus, the rolling elements	$E$	210 000	[MPa]	210 000	[MPa]
Poisson ratio of the rings	$\mu$	0.3	[-]	0.3	[-]
Poisson ratio of the rolling elements	$\mu$	0.3	[-]	0.3	[-]

In accordance with the formulas stated in the chapter Bearing stiffness, the bearing element contact stiffness calculation will be presented based on the bearing geometry dimensions stated above. For the bearing 7304 BE-2RZP it holds:

Pitch diameter  $d_e$ :

$$d_e = \frac{d_o + d_i}{2} = 36,4 \text{ mm}$$

Radius curvature for *inner-ring raceway*:

$$R_{xi} = \frac{d(d_e - d\cos\beta)}{2d_e} = 3,9 \text{ mm}$$

$$R_{yi} = \frac{R_{ri}d}{2R_{ri} - 1} = 130 \text{ mm}$$

Radius curvature for *outer-ring raceway*:

$$R_{xo} = \frac{d(d_e + d\cos\beta)}{2d_e} = 6,1 \text{ mm}$$

$$R_{yo} = \frac{R_{ro}d}{2R_{ro} - 1} = 88,3 \text{ mm}$$

Radius ratio for *inner-ring raceway*:

$$\alpha_{ri} = \frac{R_{yi}}{R_{xi}} = 32,93$$

Radius ratio for *outer-ring raceway*:

$$\alpha_{ro} = \frac{R_{yo}}{R_{xo}} = 14,59$$

Ellipticity ratio for *inner-ring raceway* and *outer-ring raceway*:

$$k_i = \alpha_{ri}^{2/\pi} = 9,24$$

$$k_o = \alpha_{ro}^{2/\pi} = 5,33$$

Elliptical integrals for *inner-ring raceway* and *outer-ring raceway*:

$$\mathcal{F}_i = \frac{\pi}{2} + \left(\frac{\pi}{2} - 1\right) \ln\alpha_{ri} = 3,56$$

$$\mathcal{F}_o = \frac{\pi}{2} + \left(\frac{\pi}{2} - 1\right) \ln\alpha_{ro} = 3,10$$

$$\mathcal{E}_i = 1 + \frac{\pi - 2}{2\alpha_{ri}} = 1,016$$

$$\mathcal{E}_o = 1 + \frac{\pi - 2}{2\alpha_{ro}} = 1,041$$

Effective Young's modulus of the contact:

$$E' = \frac{2}{\frac{1-\mu_a^2}{E_a} + \frac{1-\mu_b^2}{E_b}} = 230\,770 \text{ MPa}$$

Contact stiffness for *inner-ring raceway*:

$$K_{1.5i} = \pi k_i E' \left( \frac{2\mathcal{E}_i R_i}{9\mathcal{F}_i} \right)^{1/3} = 29\,316/m$$

Contact stiffness for *outer-ring raceway*:

$$K_{1.5o} = \pi k_o E' \left( \frac{2\mathcal{E}_o R_o}{9\mathcal{F}_o} \right)^{1/3} = 26\,457 \text{ N/m}$$

Resulting contact stiffness of the rolling element with the bearing rings is:

$$K_{1.5} = \frac{1}{\{[K_{1.5i}]^{2/3} + [K_{1.5o}]^{2/3}\}^{3/2}} = 9.838 \cdot 10^9 \text{ N/m}$$

For the bearing 7301 BE-2RZP, the calculation is processed in analogous way, the resulting stiffness of the rolling element is:

$$K_{1.5} = \frac{1}{\{[K_{1.5i}]^{2/3} + [K_{1.5o}]^{2/3}\}^{3/2}} = 8.763 \cdot 10^9 \text{ N/m}$$

Obtained values of the bearing element contact stiffness will be used further in the rotor analysis.

### 9.1.2. Analysis setting

The analysis in the program Rotor Shaft Solver was set in the following way:

Table 9.3: Settings of the inputs in the Rotor Shaft Solver

Material panel		Unit
Gravity	checked	
Young modulus	210 000	[MPa]
Density	7850	[kg · m <sup>3</sup> ]
Boundary conditions Loose-Loose		
Speed Range		
Lower bound	1000	[rpm]
Upper bound	200 000	[rpm]
Step	1000	[rpm]

The bearing element contact stiffness calculation stated in the previous section are done via panel *Bearing Parameters* as a callback to the input parameters as the figure below illustrates.

**Bearing Parameters**

Bearing Type:

**Material Properties - Rolling element**

Young modulus E [MPa]:

Poisson ratio  $\mu$  [-]:

**Material Properties - Ring raceway**

Young modulus E [MPa]:

Poisson ratio  $\mu$  [-]:

**Geometry dimensions**

Outer-race diameter  $d_o$  [mm]:

Inner-race diameter  $d_i$  [mm]:

Element diameter  $d$  [mm]:

Number of rolling element  $Z$  [-]:

Contact angle  $\beta$  [°]:

Preload  $P$  [N]:

Radial Load  $w$  [N]:

Element length  $l$  [mm]:

Calculate Result Stiffness [N/m]

Save Bearing Load Bearing

(a)

**Bearing Parameters**

Bearing Type:

**Material Properties - Rolling element**

Young modulus E [MPa]:

Poisson ratio  $\mu$  [-]:

**Material Properties - Ring raceway**

Young modulus E [MPa]:

Poisson ratio  $\mu$  [-]:

**Geometry dimensions**

Outer-race diameter  $d_o$  [mm]:

Inner-race diameter  $d_i$  [mm]:

Element diameter  $d$  [mm]:

Number of rolling element  $Z$  [-]:

Contact angle  $\beta$  [°]:

Preload  $P$  [N]:

Radial Load  $w$  [N]:

Element length  $l$  [mm]:

Calculate Result Stiffness [N/m]

Save Bearing Load Bearing

(b)

Figure 9.4: Calculation of the bearing contact stiffness in Rotor Shaft Solver, (a) SKF 7304 BE-2RZP , (b) SKF 7301 BE-2RZP

Through the panels *Element Selection* and *Element Parameters* the rotor elements sequence was defined, depicted in the following figure.

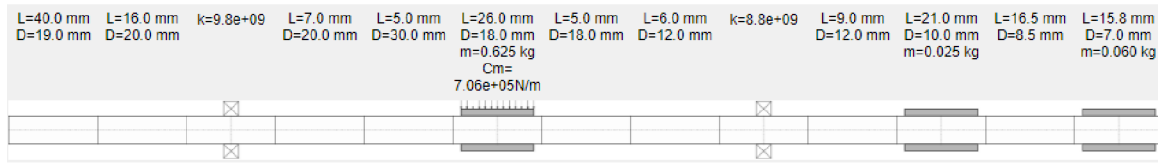


Figure 9.5: Solved rotor in scheme from program Rotor Shaft Solver

### 9.1.3. Obtained results

Deflection curve obtained in the program is plotted in the figure below.

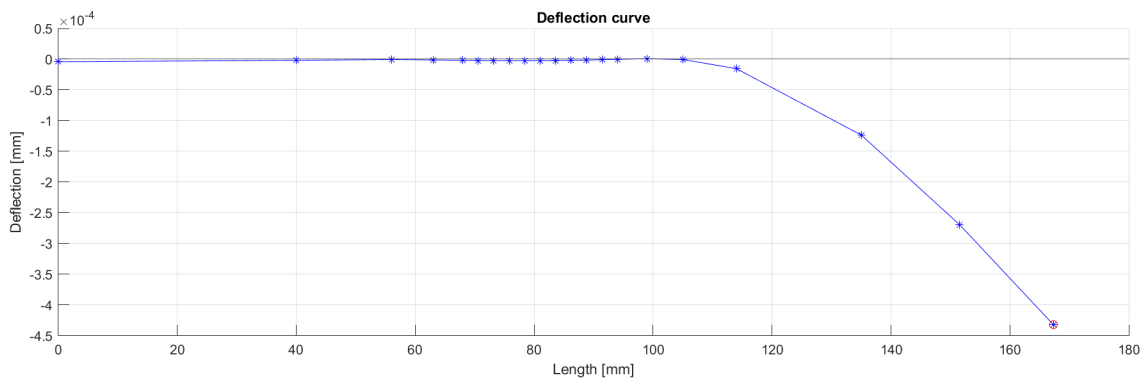


Figure 9.6: Computed deflection curve

Critical speed curve in the given range is plotted in the figure below.

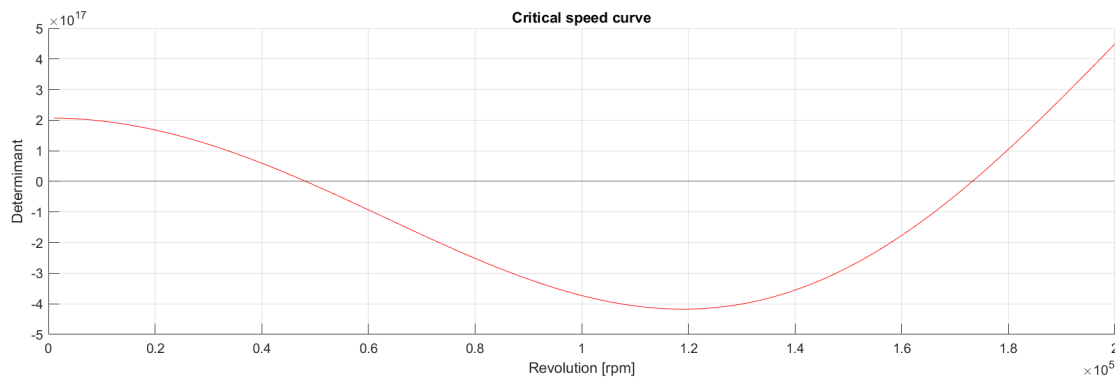


Figure 9.7: Computed curve of critical speed

With the bisection method there were located two values of the critical speed in the specified range. The values correspond to the intersections of the curve with the horizontal axis, when determinant of the global critical speed of the transfer matrix is zero. This is in accordance with the theory about the transfer matrix method for critical speed.

- First critical speed    48 234    [rpm]
- Second critical speed   173 266    [rpm]

## Bearing Results

In the panel *Bearing Results*, the table with the following results is available:

Table 9.4: Obtained bearing results, from static rotor analysis

	Reaction [N]	Deflection [mm]	Stiffness [N/m]
SKF 7304 BE-2RZP	4.6984	$4.7759 \cdot 10^{-7}$	$9.8378 \cdot 10^9$
SKF 7301 BE-2RZP	4.9541	$5.6530 \cdot 10^{-7}$	$8.7637 \cdot 10^9$

The values of the force reaction are further used in the analysis of the frictional heat loss induced in the chosen bearings. For the SKF 7304 BE-2RZP the following input parameters are required.

Table 9.5: SKF 7304 BE-2RZP power loss analysis parameters

Parameter		Value	Unit
Radial load	$F_r$	4.698	[N]
Axial load	$F_a$	0	[N]
Bore diameter	$d_b$	20	[mm]
Friction factor	$\mu$	0.002	[-]
Revolution	$n$	1500	[rpm]
Load capacity	$C_0$	9500	[N]
Radial load factor	$X$	0.35	[-]
Axial load factor	$Y$	0.26	[-]
Limiting value	$e$	1.14	[-]

In accordance with the formulas in the chapter Power losses the friction momentum can be estimated as follows, for the radial load it holds:

$$\frac{F_a}{F_r} < e$$

$$P = F_r = 4.698$$

For the resulting friction momentum it holds:

$$M_F = 0.5 \cdot \mu \cdot P \cdot d_b = 0.094 \text{ Nmm}$$

For illustration it is considered the influence of the bearing lubrication, the input parameters are gathered in the table below. The value of kinematic viscosity was selected in accordance with the SKF catalogue, when the grease lubrication is considered, the appropriate lubrication factor  $f_L = 2$  is chosen from the table in appendix Frictional coefficients.

Table 9.6: SKF 7304 BE-2RZP lubrication parameters

Parameter		Value	Unit
Kinematic viscosity	$\nu$	96	[mm <sup>2</sup> /s]
Lubrication factor	$f_L$	2	[-]
Pitch diameter	$d_m$	36	[mm]

The lubricant friction momentum can be calculated with the following formula:

$$M_L = 10^{-7} \cdot f_L \cdot (\nu \cdot n)^{2/3} \cdot d_m^3 = 25.636 \text{ Nmm}$$

The total power loss generated in the bearing SKF 7304 BE-2RZP is determined as it follows.

$$P_{diss} = (M_F + M_L) \cdot \frac{2\pi \cdot n}{60} = 4.024 \text{ W}$$

For the second bearing SKF 7301 BE-2RZP the process to estimate the power loss is analogous.

Table 9.7: SKF 7301 BE-2RZP power loss analysis parameters

Parameter		Value	Unit
Radial load	$F_r$	4.954	[N]
Axial load	$F_a$	0	[N]
Bore diameter	$d_b$	12	[mm]
Friction factor	$\mu$	0.002	[-]
Revolution	$n$	1500	[rpm]
Load capacity	$C_0$	5000	[N]
Radial load factor	$X$	0.35	[-]
Axial load factor	$Y$	0.26	[-]
Limiting value	$e$	1.14	[-]

In accordance with the formulas for the friction momentum it can be estimated, for the radial load:

$$\frac{F_a}{F_r} < e$$

$$P = F_r = 4.954$$

The resulting friction moment:

$$M_F = 0.5 \cdot \mu \cdot P \cdot d_b = 0.0594 \text{ Nmm}$$

Here it is again considered the influence of the bearing lubrication. The input parameters, gathered in the table, they are obtained in the same way as in the previous case.

Table 9.8: SKF 7301 BE-2RZP lubrication parameters

Parameter		Value	Unit
Kinematic viscosity	$\nu$	96	[mm <sup>2</sup> /s]
Lubrication factor	$f_L$	2	[-]
Pitch diameter	$d_m$	24	[mm]

The lubricant friction momentum can be calculated with the following formula:

$$M_L = 10^{-7} \cdot f_L \cdot (\nu \cdot n)^{2/3} \cdot d_m^3 = 8.08 \text{ Nmm}$$

The total power loss generated in the bearing SKF 7304 BE-2RZP is determined as it follows.

$$P_{diss} = (M_F + M_L) \cdot \frac{2\pi \cdot n}{60} = 1.279 \text{ W}$$

## 9.2. Influence of the bearing stiffness

As was mentioned above in the text, there exist several approaches to estimate the bearing stiffness. So far used approach based on the Hertz's elastic contact theory is the most simplistic. However, such model assumes an extreme case, when only single rolling element is subjected to the radial load. More realistic model can be explained as follows.

Bearing radial load is distributed among the rolling elements, as the figure 9.8 illustrates.

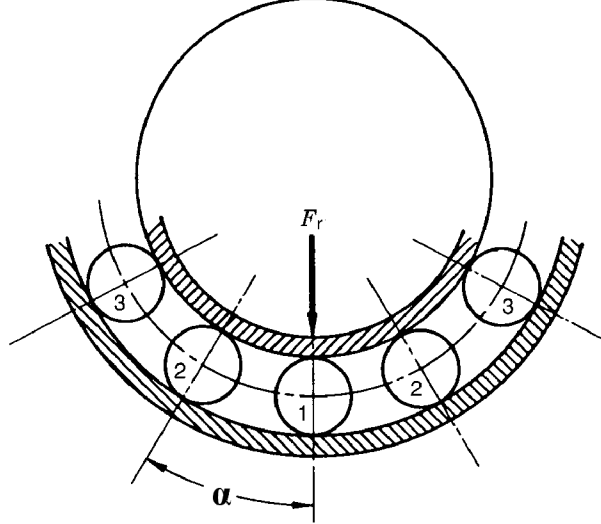


Figure 9.8: Radial load distribution [13]

Total radial force  $F_r$  equals the sum of the supports provided by the individual rolling elements, expressed by equation [13]:

$$F_r = Q_1 + 2 \cdot Q_2 \cdot \cos(\alpha) + 2 \cdot Q_3 \cdot \cos(\alpha) \dots \quad (9.1)$$

Here, a number of rolling elements  $Z$  is considered and  $\alpha$  denotes angle between the rolling elements,  $2\pi/Z$ , and  $Q_i$  is the force loading an individual rolling element.

From the general load-deflection formula 5.1, stated in the chapter Bearing stiffness, for ball bearing it holds  $Q_2/Q_1 = (\delta_2/\delta_1)^{3/2}$ , respectively  $Q_2/Q_1 = (\cos(\alpha))^{3/2}$ . After that, the equation (9.1) becomes [13]:

$$F_r = Q_1 \cdot (1 + 2 \cdot (\cos(\alpha))^{5/2} + 2 \cdot (\cos(2\alpha))^{5/2} \dots) \quad (9.2)$$

Analogous idea can be considered for rolling element leads to formula [13]:

$$F_r = Q_1 \cdot (1 + 2 \cdot (\cos(\alpha))^{1.9/0.9} + 2 \cdot (\cos(2\alpha))^{1.9/0.9} \dots) \quad (9.3)$$

The brackets of the equations above express the radial load distribution in the bearing, it can be observed the distribution depends only on the number of the rolling elements  $Z$  [13]. Further, it can be determined the maximum normal loading for the rolling element, with the influence of the contact angle  $\beta$ , expressed by the formula [13]:

$$Q_{max} = \frac{5 \cdot F_r}{Z \cdot \cos(\beta)} \quad (9.4)$$

After the maximal load for an individual rolling element has been determined. The individual deflection at inner and outer ring raceways can be obtained, from the load-deflection formula 5.1 in the form  $\delta \sim Q_{max}^{2/3}$ , for the elliptic contact, and in the form  $\delta \sim Q_{max}^{1/0.9}$  for rectangular contact, respectively. By sum of individual rolling elements radial displacement radial stiffness can be established.

The considerations stated above are the basis for more detailed calculations stated in the article [18], and [19] presenting established analytical formulas for certain rolling element bearing. Only the resulting analytical formulas for the bearing stiffness are presented here, adopted from the article [18].

The final formula for ball bearing radial stiffness is:

$$K = 0.3743 \cdot (K_{1.5} \cdot Z)^{2/3} \cdot (\cos\beta)^{5/3} \cdot F_r^{1/3} \quad (9.5)$$

The final formula for roller bearing radial stiffness is:

$$K = 0.2784 \cdot (K_1 \cdot Z)^{0.9091} \cdot (\cos\beta)^{1.09091} \cdot F_r^{0.0909} \quad (9.6)$$

Here,  $K_{1.5}$ , and  $K_1$  denotes the element contact stiffness for ball bearing, and for roller bearing, respectively. Further the  $Z$  denotes the number of rolling elements, and the  $F_r$  denotes the the bearing radial load.

It observes from the formulas above, that radial load has to be known for the bearing stiffness calculation. Following section presents procedure to do such computations in the practise.

### 9.3. Improved rotor analysis

Consider the same rotor as at the beginning of this chapter, with the parameters grouped in the table 9.1. As the bearing stiffness it was considered the estimated contact stiffness. The following table gathers the necessary parameters for the computations of the bearing stiffness in accordance with the formula (9.3) from the previous section. Stated force reactions are taken from the previous static rotor analysis, bearing element contact stiffness as well:

Table 9.9: Inputs for the calculation of the bearing stiffness

	Reaction [N]	Contact stiffness [N/m]	Rolling elements Z
SKF 7304 BE-2RZP	4.6984	$9.8378 \cdot 10^9$	9
SKF 7301 BE-2RZP	4.9541	$8.7637 \cdot 10^9$	8

For bearing SKF 7304 BE-2RZP, it holds:

$$K = 0.3743 \cdot (K_{1.5} \cdot Z)^{2/3} \cdot (\cos\beta)^{5/3} \cdot F_r^{1/3} = 7.9870 \cdot 10^6 \text{ N/m}$$

For bearing SKF 7301 BE-2RZP, it holds:

$$K = 0.3743 \cdot (K_{1.5} \cdot Z)^{2/3} \cdot (\cos\beta)^{5/3} \cdot F_r^{1/3} = 6.9580 \cdot 10^6 \text{ N/m}$$

Since new estimated stiffness values are three orders smaller, compared to the original defined rotor, the effect of the different stiffness values to analysis result can be expected. The bearings in the original rotor system were replaced with the new established values and the static analysis and the critical speed computation were made again with use of the program Rotor Shaft Solver. The rotor is depicted below:

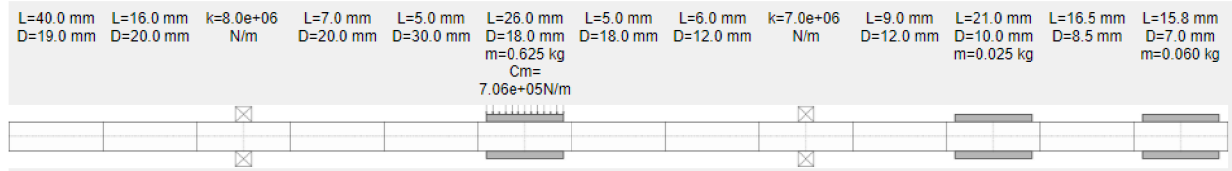


Figure 9.9: Solved rotor in scheme with the updated support stiffness values

The following table collects the static calculation results of the origin analysis and the analysis with updated stiffness values.

Table 9.10: Comparison of resulting bearing reactions and deflection

	Stiffness [N/m]	Reaction [N]	Deflection [mm]
SKF 7304 BE-2RZP	$9.8378 \cdot 10^9$	4.6984	$4.7759 \cdot 10^{-7}$
SKF 7301 BE-2RZP	$8.7637 \cdot 10^9$	4.9541	$5.6530 \cdot 10^{-7}$
SKF 7304 BE-2RZP	$7.9870 \cdot 10^6$	4.9334	$6.1767 \cdot 10^{-4}$
SKF 7301 BE-2RZP	$6.9580 \cdot 10^6$	5.2024	$7.4768 \cdot 10^{-4}$

From the values of the deflection, the impact of the updated stiffness is evident, since the deflection is larger compared to the previous case of the rotor when stiffer bearings had been considered.

Results comparison should be done also for critical speed calculation. Following table give a comparison of obtained critical speed with respect to different spring support stiffness values.

Table 9.11: Comparison of critical speed

	Bearing stiffness		Units
	Original	Updated	
SKF 7304 BE-2RZP	$9.8378 \cdot 10^9$	$7.9870 \cdot 10^6$	[N/m]
SKF 7301 BE-2RZP	$8.7637 \cdot 10^9$	$6.9580 \cdot 10^6$	[N/m]
Critical speed			
First critical speed	48 234	26 359	[rpm]
Second critical speed	173 266	37 984	[rpm]
Third critical speed	-	73 547	[rpm]

The results stated in the tables above implies the support stiffness values have a significant effect to resulting critical speed values. The outcome corresponds to generally known assumptions, the higher the stiffness of the system is, the higher the natural frequencies, respectively critical speeds, are, and vice versa.

## 9.4. Validation

Use of stated formulas for bearing stiffness (9.3), and (9.6) has been validated by the following comparison. From research stated in [20] results of bearing stiffness estimation has been adopted. For bearing SKF 6205 had been estimated the radial stiffness via finite element simulation as  $K_r = 9.5 \cdot 10^7 \text{ N/m}$ , corresponding to radial load  $F_r = 894 \text{ N}$ . Following table gathers necessary parameters, for the computations:

Table 9.12: Parameters of bearing SKF 6205

Parameter	SKF 6205	
	Value	Unit
Outer-raceway diameter	$d_o$	46,3 [mm]
Inner-raceway diameter	$d_i$	34.4 [mm]
Element diameter	$d$	7.9 [mm]
Pitch diameter	$d_e$	38.5 [mm]
Outer diameter	$D$	52 [mm]
Contact angle	$\beta_f$	0 [°]
Number of rolling elements	$Z$	9 [-]
Young modulus, the rings	$E$	210 000 [MPa]
Young modulus, the rolling elements	$E$	210 000 [MPa]
Poisson ratio of the rings	$\mu$	0.3 [-]
Poisson ratio of the rolling elements	$\mu$	0.3 [-]

Using the developed *Rotor Shaft Solver* in the panel *Bearing Parameters* bearing element contact stiffness has been computed as  $K_{1.5} = 8.745 \cdot 10^9 \text{ N/m}$ .

The screenshot shows a software interface titled "Bearing Parameters". It is divided into several sections:

- Bearing Type:** A dropdown menu set to "Ball Bearing".
- Material Properties - Rolling element:**
  - Young modulus E [MPa]: 2.1e+05
  - Poisson ratio  $\mu$  [-]: 0.3
- Material Properties - Ring raceway:**
  - Young modulus E [MPa]: 2.1e+05
  - Poisson ratio  $\mu$  [-]: 0.3
- Geometry dimensions:**
  - Outer-race diameter  $d_o$  [mm]: 46.3
  - Inner-race diameter  $d_i$  [mm]: 34.4
  - Element diameter  $d$  [mm]: 7.9
  - Number of rolling element  $Z$  [-]: 9
  - Contact angle  $\beta$  [°]: 0
  - Preload  $P$  [N]: 0
  - Radial Load  $w$  [N]: 0
  - Element length  $l$  [mm]: 0

At the bottom, there are three buttons: "Calculate", "Save Bearing", and "Load Bearing". The "Calculate" button is active, and the "Result Stiffness [N/m]" field displays the value "8.745e+09".

Figure 9.10: SKF 6205 contact stiffness estimation

By substitution of available parameters into equation (9.3), the stiffness of the SKF 6205 is estimated:

$$K = 0.3743 \cdot (K_{1.5} \cdot Z)^{2/3} \cdot (\cos\beta)^{5/3} \cdot F_r^{1/3} = 6.622 \cdot 10^7 \text{ N/m}$$

For comparison has been used available software MESYS, suitable also for rolling bearing analysis. The SKF 6205 bearing has been defined in the program in accordance with the parameters stated in table 9.12, the radial load has been set on the value from stated FEM analysis  $F_r = 894 \text{ N}$ .

Corresponding radial deflection has been computed as  $\delta_r = 0.013 \text{ mm}$ . Using in general known formula for load-deflection relation the stiffness has been estimated, as follows:

$$K = \frac{F_r}{\delta_r} = 6.85 \cdot 10^7 \text{ N/m}$$

Obtained values show, the result from stated formula (9.3) is almost the same as result achieved with MESYS Rolling Bearing Calculation. However, these values are slightly different from the outcomes, of the FEM analysis. Since the order of the values is the same  $10^7 \text{ N/m}$ , it can be concluded, the stated analytical formulas approach, based on Hertzian contact theory, can be used in practise for rough stiffness estimation.

## 9.5. Software improvement

In accordance with the conclusion in the end of the previous section, there have been made certain improvements in the developed program *Rotor Shaft Solver*. The scheme 9.11 illustrates the iterative work-flow in the improved rotor solver.

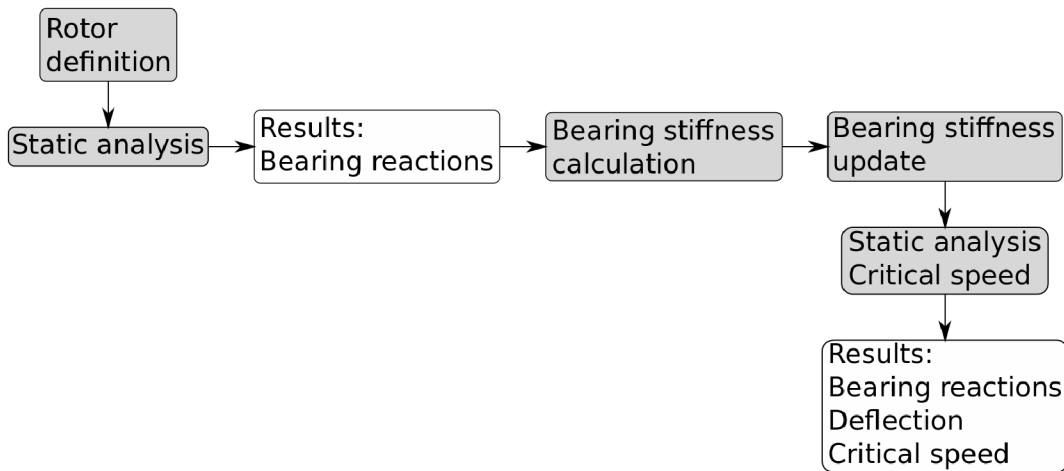


Figure 9.11: Scheme of an iterative work-flow in the Rotor Shaft Solver

Let suppose user aims to analyse rotor system, when the bearing support stiffness is not exactly known. First, the rotor should be defined with the supports considered as rigid. That means the value of the spring support stiffness should be at least  $k = 10^{12} \text{ N/m}$ . As the rotor is defined, the static analysis using the *Deflection* push button is processed. After that, the table in the panel *Bearing Results* is filled in as the figure 9.12 shows.

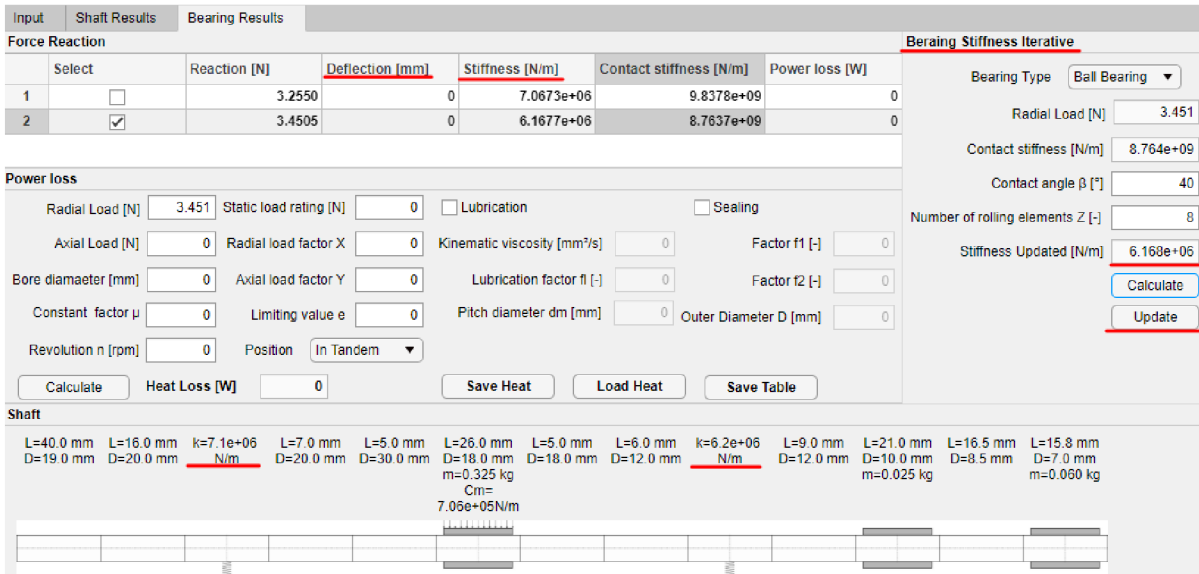


Figure 9.12: Improved Bearing Results panel

If the certain bearing is selected using the checkbox in the first column, user can calculate the bearing contact stiffness using the *Bearing Parameters* in the *Input* tab, in the same way as in the examples stated earlier in the text. With the button *Upload* the estimated value is uploaded in the table in corresponding selected row in the column *Contact Stiffness*. This step is repeated for all supports of the rotor. There exists the option to fill the contact stiffness directly in the table, since the column *Contact Stiffness* is editable. After the contact stiffness has been estimated for all bearings, the calculation of the stiffness based in the formulas (9.3), and (9.6) can be done.

For this calculation servers the panel *Bearing stiffness iterative* located next to the *Bearing results* table. The check-boxes in the first column is used again to to select the bearing. As a callback the force reaction and the contact stiffness are uploaded in the fields *Radial load* and the *Contact stiffness*, in the panel *Bearing Stiffness Iterative*. Only the contact angle, and number of rolling elements are required as the input, for selected bearing. After that the stiffness can be calculated, the value appears in the field *Updated stiffness*. When the button *Update* is pressed, the corresponding spring support will be replaced with the new stiffness value. This step has to be again repeated for all bearings. One more fact has to reminded. As the stiffness has been updated, data about the deflection curve and the critical speed are deleted. This can be recognized since the values of the deflection in the table are exactly 0. To plot the deflection curve, or get the critical speed, the buttons *Deflection*, or *Critical Speed* need to be used again. As a result, new data about the deflection, or critical speed are obtained and filled in the table.

### 9.5.1. Illustrative example

Finally is presented an illustrative example of the iterative rotor analysis procedure. Consider again the rotor from the previous section, when the initial spring support stiffness is set as  $k = 10^{12} \text{ N/m}$ , for both bearings. The contact stiffness values are the same, as estimated in the previous sections:  $9.8378 \cdot 10^9$ , respectively  $8.7637 \cdot 10^9$ .

Table below shows comparison of three iterations computed in the Rotor Shaft Solver. Values of critical speed in first and second iteration implies that first, or second iteration helps to get be more accurate results with respect to true critical speed, of solved rotor system.

Table 9.13: Iteration comparison

Bearing	Quantity	Units	Iteration		
			Initial	First	Second
SKF 7304 BE-2RZP	Reaction	[N]	4.6984	4.9334	4.9294
SKF 7301 BE-2RZP			4.941	5.2024	5.1982
SKF 7304 BE-2RZP	Support stiffness	[N/m]	$10^{12}$	$7.987 \cdot 10^6$	$8.118 \cdot 10^6$
SKF 7301 BE-2RZP			$10^{12}$	$6.958 \cdot 10^6$	$7.0723 \cdot 10^6$
SKF 7304 BE-2RZP	Power loss	[W]	4.0534	4.054	4.054
SKF 7301 BE-2RZP			1.1218	1.2128	1.2127
Rotor critical speed		[rpm]	48 234	26 359	26 547
			173 266	37 984	38 266
				73 547	73 672

Table data show, the iterative procedure of the analysis has importance specially for critical speed results, if the bearing stiffness is not precisely known at the beginning of the analysis. Since the values of the bearing reactions only slightly differ during the iteration, there is not significant difference in induced bearing heat loss.

# 10. Summary

This master thesis has been dedicated to practical application of rotor system modeling methods. Based on the research especially in field of beam analysis methods, bearing contact stiffness computation, and bearing friction phenomenon, has been developed a simple software gathering the theoretical findings with aim to make the rotor analysis as simple as possible for practical performances.

The developed software has been illustrated with practical solving of given rotor system. Further followed a discussion about the impact of different bearing stiffness estimation approaches to final outcomes of the analysis. Based on the conclusion arising from the result comparison has been made an improvement in the developed software. The upgrade is focused on more precise results to be obtained especially with respect to rotor critical speed. The enhanced accuracy is gained, since the procedure of the analysis has to be iterative. The comparison in the final section shows, at least one iteration should be made to get closer to true critical speed of the rotor. However, it has to be reminded the used approach is based on simple analytical formula, based on certain simplification assumption for Hertz's elastic contact theory. For more complex bearing system, or in cases with greater accuracy required, the bearing manufacturer should be consulted in order to obtain the bearing stiffness values reflecting the geometry of particular bearing design, and other specific operational conditions.

Further, the possible computation of induced bearing heat loss can be useful in potential design of new rolling-element bearings based on development of new material for the manufacturing. For instance ceramic materials disposing for example greater abrasion resistance compared to steel bearings elements can be used with potential improvement of the bearings' lifespan.

The bearing lifespan analysis can be one of the future improvements of the developed software. Another limitation of the solver is the the iterative process of the bearing stiffness estimation and critical speed analysis has to be performed manually and it is only up to user how many iterations will be performed.

The last suggestion to improve the built program is more detail analysis of impact of the magnetic field in solved rotor system. In the developed software the magnetic field in the machine is represented only with magnetic pull stiffness considered as a constant in the calculation. It could be in more detail explored mutual influence of the varying bearing stiffness leading to different deflections even between rotor and stator, and consequently arising magnetic forces. And vice versa, varying values of magnetic pull stiffness could affect final bearing load, important for iterative bearing stiffness calculation with the impact to resulting critical speed.

# 11. List of appendix and used software

## Appendix

- Transfer matrices
- Frictional coefficients

## Electronic Appendix

- CAD geometry 7304 BE-2RZP
- CAD geometry 7301 BE-2RZP
- MATLAB script of the developed program *RotorShaftSolver.m*

## Used software

- MATLAB R2020b; License: 40874381, MATLAB (Individual)
- Inkscape 0.92.4 (5da689c313, 2019-01-14)
- MESYS Rolling Bearing Calculation; Version: 08-2021b (x64); Demoverision
- Overleaf, Online LaTeX Editor



# Bibliography

- [1] VRBKA, Jan. *PRUŽNOST A PEVNOST I: Učební text*. Brno: Fakulta strojního inženýrství VUT, 2012.
- [2] PUCHMAJER, Pavel, Jan ŘEZNÍČEK a Vladimír ŠVEHLA. *Pružnost a pevnost pro VS I*. Praha: ČVUT, 1993, 73 s. ISBN 80-01-00993-9.
- [3] PILKEY, Walter D. *Formulas for stress, strain, and structural matrices*. 2. ed. Norwich: NY: Knovel, 2007. ISBN 978-160-1190-451.
- [4] VLACH, Radek. *Transfer matrix method*. Brno, 2022.
- [5] ČERMÁK, Libor a Rudolf HLAVIČKA. *Numerické metody*. Vyd. 2. Brno: Akademické nakladatelství CERM, 2008, 110 s. : il. ; 30 cm. ISBN 978-80-214-3752-4.
- [6] *Bisection method for root finding* [online]. [cit. 2022-03-02]. Available: <https://x-engineer.org/bisection-method/>
- [7] ELDÉN, Lars, Linde WITTMAYER-KOCH a Hans Bruun NIELSEN. *Introduction to Numerical Computation: analysis and MATLAB illustrations*. Studentlitteratur, 2004. ISBN 8188689254.
- [8] DONÁT, Martin. Computational Modelling of the Unbalanced Magnetic Pull by Finite Element Method. *Procedia engineering* [online]. Elsevier, 2012, **48**, 83-89 [cit. 2022-02-21]. ISSN 1877-7058. Available:: doi:10.1016/j.proeng.2012.09.489
- [9] KIM, Heesoo, Janne NERG, Tuhin CHOUDHURY a Jussi T SOPANEN. Rotordynamic Simulation Method of Induction Motors Including the Effects of Unbalanced Magnetic Pull. *IEEE access* [online]. Piscataway: IEEE, 2020, **8**, 21631-21643 [cit. 2022-02-21]. ISSN 2169-3536. Available:: doi:10.1109/ACCESS.2020.2968915
- [10] KIM, Heesoo, Eerik SIKANEN, Janne NERG, Teemu SILLANPAA a Jussi T SOPANEN. Unbalanced Magnetic Pull Effects on Rotordynamics of a High-Speed Induction Generator Supported by Active Magnetic Bearings - Analysis and Experimental Verification. *IEEE access* [online]. Piscataway: IEEE, 2020, **8**, 212361-212370 [cit. 2022-02-21]. ISSN 2169-3536. Available: doi:10.1109/ACCESS.2020.3039629
- [11] KIM, Heesoo, Atte POSA, Janne NERG, Janne HEIKKINEN a Jussi T SOPANEN. Analysis of Electromagnetic Excitations in an Integrated Centrifugal Pump and Permanent Magnet Synchronous Motor. *IEEE transactions on energy conversion* [online]. PISCATAWAY: IEEE, 2019, **34**(4), 1759-1768 [cit. 2022-02-21]. ISSN 0885-8969. Available: doi:10.1109/TEC.2019.2935785
- [12] SCHMID, Steven R., Bernard J HAMROCK a Bo O. JACOBSON. *Fundamentals of machine elements*. Third edition. Boca Raton: CRC Press, 2014, xvi, 610 stran : ilustrace. ISBN 978-1-4398-9132-2.
- [13] KHONSARI, Michael M. a Richard E. BOOSER. *Applied Tribology: Bearing Design and Lubrication*. 3rd. New York: John Wiley, 2001. ISBN 0-471-28302-9.

- [14] ZHANG, Henghai, Wenku SHI, Guozheng LIU a Zhiyong CHEN. A Method to Solve the Stiffness of Double-Row Tapered Roller Bearing. *Mathematical problems in engineering* [online]. Hindawi, 2019, **2019**, 1-13 [cit. 2022-04-13]. ISSN 1024-123X. Dostupné z: doi:10.1155/2019/1857931
- [15] HERNOT, X., M. SARTOR a J. GUILLOT. Calculation of the Stiffness Matrix of Angular Contact Ball Bearings by Using the Analytical Approach. *Journal of Mechanical Design* [online]. 2000, **122**(1), 83-90 [cit. 2022-02-15]. ISSN 1050-0472. Available: doi:10.1115/1.533548
- [16] GUAY, Pascal a Ahmed. Ball Bearing Stiffness: A New Approach Offering Analytical Expressions. *European Space Mechanisms and Tribology Symposium*. 2015.
- [17] BUDYNAS, Richard Gordon a Keith J. NISBETT. *Shigley's mechanical engineering design*. 8th ed. New York: McGraw-Hill, 2006. ISBN 0-07-312193-2.
- [18] HOUPERT, L. *A Uniform Analytical Approach for Ball and Roller Bearings Calculations*. ASME J. Tribol., 1997, pp. 851—858.
- [19] GARGIULO, E. P. Jr. A simple way to estimate bearing stiffness. *Machine Design*. 1980, **52**(17), 107-110. ISSN 00249114.
- [20] GUO, Yi a Robert G. PARKER. Stiffness matrix calculation of rolling element bearings using a finite element/contact mechanics model. *Mechanism and Machine Theory* [online]. 2012, **51**, 32-45 [cit. 2022-05-19]. ISSN 0094114X. Dostupné z: doi:10.1016/j.mechmachtheory.2011.12.006

# List of Figures

2.1	Beam with denoted segments [3]	7
2.2	Beam segment at point $j$ [3]	9
3.1	Rotor eccentricity scheme [11]	14
3.2	Magnetic pull element division scheme	16
4.1	Description of the most common rolling-element bearing types [13], (a) Ball bearing, (b) Cylindrical roller bearing, (c) Tapered roller bearing, (d) Thrust ball bearing	17
4.2	Illustration of the bearing contact angle [12], (a) Unloaded ball bearing cross section, (b) Loaded ball bearing cross section with the contact angle	18
4.3	Angular-contact ball bearing, cross section detail [12]	19
4.4	Cross section scheme of tapered roller bearing with marked contact angle [12]	19
5.1	Cross section of single row ball bearing [12]	21
5.2	Designations for radii of curvature for rolling bearing races [12]	23
5.3	Preloaded paired bearing [16]	25
5.4	Deflection curve for paired bearing [16]	26
8.1	Solver layout, with filled example	31
8.2	Scheme of the rotor definition and obtained results	31
8.3	Scheme of the bearing results analysis	32
8.4	Scheme of the data save	33
8.5	Panel with for bearing stiffness estimation	35
8.6	Detail of the panel <i>Speed Range</i> and <i>Material</i>	36
8.7	Visualized shaft scheme	37
8.8	Shaft result panel	37
8.9	The panel gathering the bearing results	38
8.10	Data structure of the rotor definition saved file	40
8.11	Data structure of the bearing definition saved file	41
8.12	Data structure of the heat loss parameters saved file	42
8.13	Warning dialogue about Young modulus	44
8.14	Warning dialogue about material density	44
8.15	Warning dialogue about Speed range	44
8.16	Warning dialogue about possible singular matrix	44
8.17	Warning dialogue about missing specific parameter	45
8.18	Warning dialogue about missing rotor definition	45
8.19	Application package and install buttons location, in MATLAB window	45
9.1	Drawing scheme of the solved rotor AF 502-B	46
9.2	Scheme of the solved rotor AF 502-B for transfer matrix algorithm	46
9.3	Selected bearings geometry	48
9.4	Calculation of the bearing contact stiffness in Rotor Shaft Solver, (a) SKF 7304 BE-2RZP, (b) SKF 7301 BE-2RZP	51
9.5	Solved rotor in scheme from program Rotor Shaft Solver	52
9.6	Computed deflection curve	52
9.7	Computed curve of critical speed	52
9.8	Radial load distribution [13]	55

9.9 Solved rotor in scheme with the updated support stiffness values . . . . . 57  
9.10 SKF 6205 contact stiffness estimation . . . . . 58  
9.11 Scheme of an iterative work-flow in the Rotor Shaft Solver . . . . . 59  
9.12 Improved Bearing Results panel . . . . . 60

# List of Tables

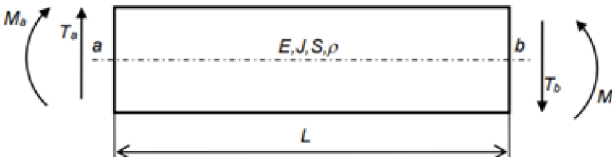
5.1	Simplified elliptic integrals contact equations [12]	22
8.1	List of the element types with required parameters	34
8.2	Bearing type input parameters	35
8.3	Possible boundary conditions	36
8.4	Load friction inputs	38
8.5	Lubrication friction inputs	38
8.6	Sealing friction inputs	39
9.1	Solved rotor parameters	47
9.2	Selected bearings parameters	48
9.3	Settings of the inputs in the Rotor Shaft Solver	51
9.4	Obtained bearing results, from static rotor analysis	53
9.5	SKF 7304 BE-2RZP power loss analysis parameters	53
9.6	SKF 7304 BE-2RZP lubrication parameters	53
9.7	SKF 7301 BE-2RZP power loss analysis parameters	54
9.8	SKF 7301 BE-2RZP lubrication parameters	54
9.9	Inputs for the calculation of the bearing stiffness	56
9.10	Comparison of resulting bearing reactions and deflection	57
9.11	Comparison of critical speed	57
9.12	Parameters of bearing SKF 6205	58
9.13	Iteration comparison	61

# Transfer matrices

The following formulas show transfer matrices for certain shaft element in considered segment given by an arbitrary interval  $[a, b]$ , adopted from [4]

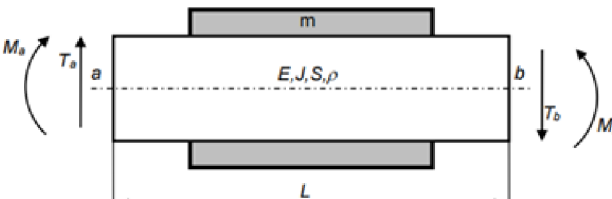
## List of transfer matrices - Static problems

- Shaft element



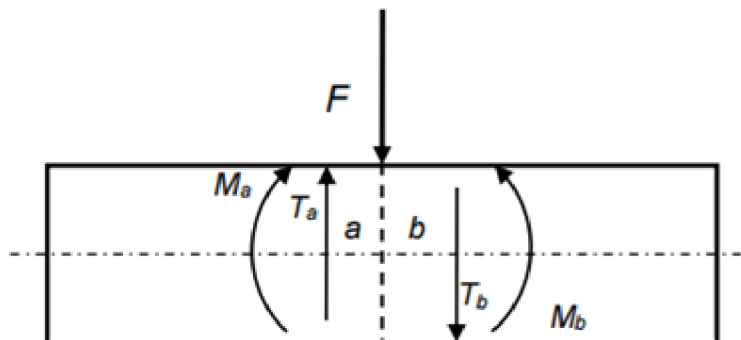
$$\begin{bmatrix} 1 & L & -\frac{L^2}{2EJ} & -\frac{L^3}{6EJ} & -\frac{S\rho g L^4}{24EJ} \\ 0 & 1 & -\frac{-L}{EJ} & -\frac{L^2}{2EJ} & -\frac{S\rho g L^3}{6EJ} \\ 0 & 0 & 1 & L & -\frac{S\rho g L^2}{2} \\ 0 & 0 & 0 & 1 & -S\rho g L \\ 0 & 0 & 0 & 0 & 1 \end{bmatrix}_{a,b}$$

- Shaft element with added mass



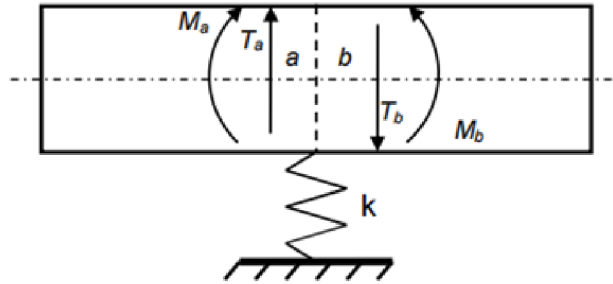
$$\begin{bmatrix} 1 & L & -\frac{L^2}{2EJ} & -\frac{L^3}{6EJ} & -\frac{(S\rho g + \frac{mg}{l})L^4}{24EJ} \\ 0 & 1 & -\frac{-L}{EJ} & -\frac{L^2}{2EJ} & -\frac{(S\rho g + \frac{mg}{l})L^3}{6EJ} \\ 0 & 0 & 1 & L & -\frac{(S\rho g + \frac{mg}{l})L^2}{2} \\ 0 & 0 & 0 & 1 & -(S\rho g + \frac{mg}{l})L \\ 0 & 0 & 0 & 0 & 1 \end{bmatrix}_{a,b}$$

- Transverse concentrated force



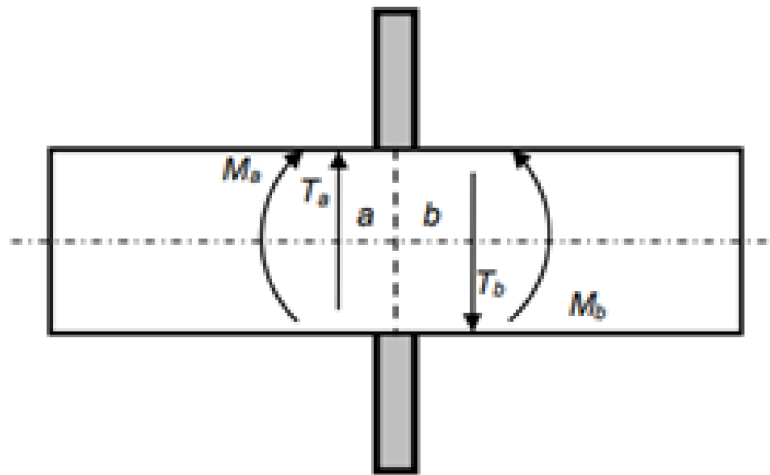
$$\begin{bmatrix} 1 & 0 & 0 & 0 & 0 \\ 0 & 1 & 0 & 0 & 0 \\ 0 & 0 & 1 & 0 & 0 \\ 0 & 0 & 0 & 1 & -F \\ 0 & 0 & 0 & 0 & 1 \end{bmatrix}_{a,b}$$

- Spring support



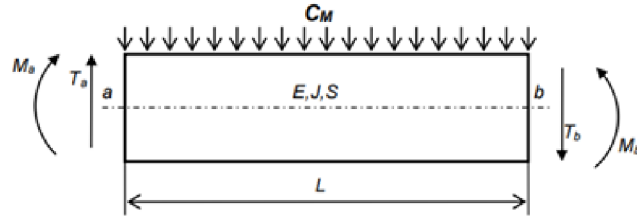
$$\begin{bmatrix} 1 & 0 & 0 & 0 & 0 \\ 0 & 1 & 0 & 0 & 0 \\ 0 & 0 & 1 & 0 & 0 \\ k & 0 & 0 & 1 & 1 \\ 0 & 0 & 0 & 0 & 1 \end{bmatrix}_{a,b}$$

- Disc



$$\begin{bmatrix} 1 & 0 & 0 & 0 & 0 \\ 0 & 1 & 0 & 0 & 0 \\ 0 & I\omega^2 & 1 & 0 & 0 \\ -m\omega^2 & 0 & 0 & 1 & 1 \\ 0 & 0 & 0 & 0 & 1 \end{bmatrix}_{a,b}$$

- Magnetic pull



- Matrix expressing discretization of magnetic pull stiffness

$$\begin{bmatrix} 1 & 0 & 0 & 0 & 0 \\ 0 & 1 & 0 & 0 & 0 \\ 0 & 0 & 1 & 0 & 0 \\ -C_m/n - 1 & 0 & 0 & 1 & 1 \\ 0 & 0 & 0 & 0 & 1 \end{bmatrix}$$

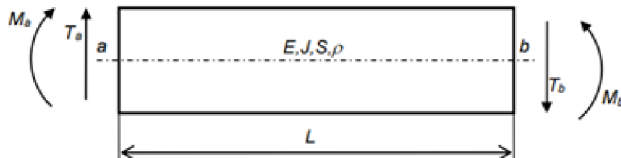
- Matrix describing discretization of shaft element

$$\begin{bmatrix} 1 & L & -\frac{(L/n)^2}{2EJ} & -\frac{(L/n)^3}{6EJ} & -\frac{S\rho g(L/n)^4}{24EJ} \\ 0 & 1 & -\frac{(L/n)}{EJ} & -\frac{(L/n)^2}{2EJ} & -\frac{S\rho g(L/n)^3}{6EJ} \\ 0 & 0 & 1 & L & -\frac{S\rho g(L/n)^2}{2} \\ 0 & 0 & 0 & 1 & -S\rho g(L/n) \\ 0 & 0 & 0 & 0 & 1 \end{bmatrix}$$

- Final matrix arises from multiplication of alternate sequence composed from last two stated above

## List of transfer matrices - Rotating elements

- Shaft element



$$\begin{bmatrix} V_1(\gamma L) & \frac{V_2(\gamma L)}{\gamma} & -\frac{V_3(\gamma L)}{\gamma^2 EJ} & -\frac{V_3(\gamma L)}{\gamma^3 EJ} \\ \gamma V_4(\gamma L) & V_1(\gamma L) & -\frac{V_2(\gamma L)}{\gamma EJ} & -\frac{V_3(\gamma L)}{\gamma^2 EJ} \\ -\gamma^2 EJ V_3(\gamma L) & -\gamma EJ V_4(\gamma L) & V_1(\gamma L) & \frac{V_2(\gamma L)}{\gamma} \\ -\gamma^3 EJ V_2(\gamma L) & -\gamma^2 EJ V_3(\gamma L) & \gamma V_4(\gamma L) & V_1(\gamma L) \end{bmatrix}_{a,b}$$

$$V_1(\gamma L) = \frac{1}{2} [\cosh(\gamma L) + \cos(\gamma L)]$$

$$V_2(\gamma L) = \frac{1}{2} [\sinh(\gamma L) + \sin(\gamma L)]$$

$$V_3(\gamma L) = \frac{1}{2} [\cosh(\gamma L) - \cos(\gamma L)]$$

$$V_4(\gamma L) = \frac{1}{2} [\sinh(\gamma L) - \sin(\gamma L)]$$

$$\gamma = \sqrt[4]{\frac{\rho S \Omega^2}{EJ}}$$

- Shaft element with added mass

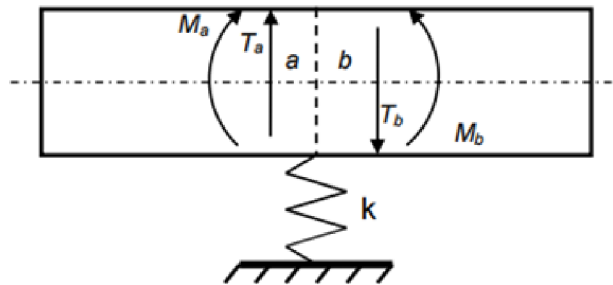
The transfer matrix formula is the same as in the previous case with the only difference for density in the formula for coefficient  $\gamma$ .

$$\rho_m = \rho + \frac{m}{S \cdot L}$$

- Transverse concentrated force

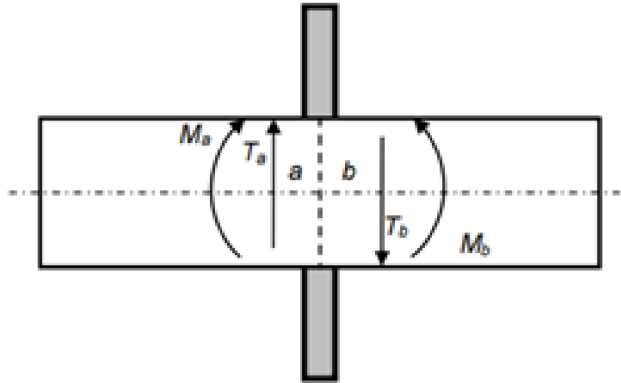
$$\begin{bmatrix} 1 & 0 & 0 & 0 \\ 0 & 1 & 0 & 0 \\ 0 & 0 & 1 & 0 \\ 0 & 0 & 0 & 1 \end{bmatrix}_{a,b}$$

- Spring support of rotating shaft



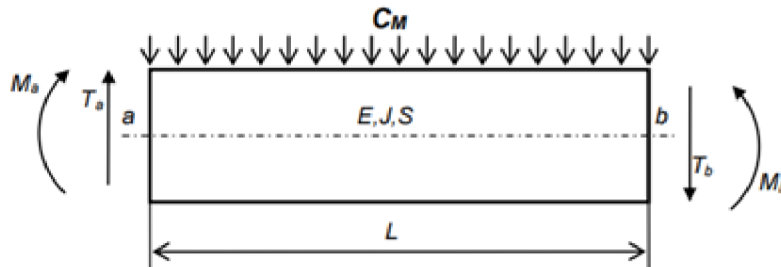
$$\begin{bmatrix} 1 & 0 & 0 & 0 \\ 0 & 1 & 0 & 0 \\ 0 & 0 & 1 & 0 \\ k & 0 & 0 & 1 \end{bmatrix}_{a,b}$$

- Disc



$$\begin{bmatrix} 1 & 0 & 0 & 0 & 0 \\ 0 & 1 & 0 & 0 & 0 \\ 0 & I\Omega^2 & 1 & 0 & 0 \\ -m^2 & 0 & 0 & 1 & 1 \\ 0 & 0 & 0 & 0 & 1 \end{bmatrix}_{a,b}$$

- Magnetic pull



- Matrix expressing discretization of magnetic pull stiffness

$$\begin{bmatrix} 1 & 0 & 0 & 0 & 0 \\ 0 & 1 & 0 & 0 & 0 \\ 0 & 0 & 1 & 0 & 0 \\ -C_m/n - 1 & 0 & 0 & 1 & 1 \\ 0 & 0 & 0 & 0 & 1 \end{bmatrix}$$

- Matrix describing discretization of shaft element

$$\begin{bmatrix} V_1(\gamma L/n) & \frac{V_2(\gamma L)}{\gamma} & -\frac{V_3(\gamma L/n)}{\gamma^2 EJ} & -\frac{V_3(\gamma L/n)}{\gamma^3 EJ} \\ \gamma V_4(\gamma L/n) & V_1(\gamma L) & -\frac{V_2(\gamma L/n)}{\gamma EJ} & -\frac{V_3(\gamma L/n)}{\gamma^2 EJ} \\ -\gamma^2 EJV_3(\gamma L/n) & -\gamma EJV_4(\gamma L/n) & V_1(\gamma L/n) & \frac{V_2(\gamma L/n)}{\gamma^2 EJ} \\ -\gamma^3 EJV_2(\gamma L/n) & -\gamma^2 EJV_3(\gamma L/n) & \gamma V_4(\gamma L) & V_1(\gamma L/n) \end{bmatrix}$$

$$V_1(\gamma L) = \frac{1}{2} [\cosh(\gamma L) + \cos(\gamma L)]$$

$$V_2(\gamma L) = \frac{1}{2} [\sinh(\gamma L) + \sin(\gamma L)]$$

$$V_3(\gamma L) = \frac{1}{2} [\cosh(\gamma L) - \cos(\gamma L)]$$

$$V_4(\gamma L) = \frac{1}{2} [\sinh(\gamma L) - \sin(\gamma L)]$$

$$\gamma = \sqrt[4]{\frac{\rho S \Omega^2}{EJ}}$$

- Final matrix arises from multiplication of alternate sequence composed from last two stated above

# Frictional coefficients

In this appendix are stated tables for bearing friction coefficients, which are discussed in chapter Power losses. Data are adopted from [13].

Coefficient of friction for rolling element bearings	
Bearing type	Coefficient of friction, $\mu$
Deep-groove ball bearings	0.0015
Self-aligning ball bearings	0.0010
Angular-contact ball bearing	
Single row	0.0020
Double row	0.0024
Cylindrical roller bearings	
With cage	0.0011
Full complement	0.0020
Spherical roller bearings	0.0018
Taper roller bearings	0.0018
Thrust ball bearings	0.0013
Cylindrical roller thrust bearings	0.0050

Bearing type	Lubrication friction factor $f_L$			
	Grease lubrication	Oil spot lubrication	Oil bath lubrication	Vertical shaft oil jet
Deep-groove ball bearing	0.75-2	1	2	4
Self-aligning ball bearing	1.5-2	0.7-1	1.5-2	3-4
Angular-contact ball bearing				
Single row	2	1.7	3.3	6.6
Double row, bearing pair	4	3.4	6.5	13
Cylindrical roller bearing	0.6-1	1.5-2.8	2.2-4	2.2-4
Spherical roller bearing	3.5-7	1.75-3.5	3.5-7	7-14
Taper roller bearing				
Single row	3-6	6	8	8-10
Paired single row	12	6	12	16-20
Thrust ball bearing	5.5	0.8	1.5	3
Cylindrical roller bearing	9		3.5	7

Bearing design	Friction factors for bearing seals $f_1$ and $f_2$	
	$f_1$	$f_2$
Deep groove ball bearings (2RS1), self-aligning ball bearings (2RS1), angular-contact ball bearing (2RS), Y-bearings (series 17262(00)-2RS1 and 17263(00)-2RS1)	20	10
Y-bearings (all other series), needle roller bearings (2RS)	20	25
Cylindrical roller bearings, full complement (2LS)		